# Influence of initial soil moisture in a Regional Climate Model study over West Africa. Part 1: Impact on the climate mean.

Brahima KONÉ[1], Arona DIEDHIOU[1, 2], Adama Diawara[1], Sandrine Anquetin[2], N'datchoh Evelyne Touré[1], Adama Bamba[1], and Arsene Toka Kobea[1]

[1]LASMES, African Centre of Excellence on Climate Change, Biodiversity and Sustainable Agriculture / University Félix Houphouët Boigny, Abidjan, Côte d'Ivoire

[2]Univ. Grenoble Alpes, IRD, CNRS, Grenoble INP, IGE, F-38000 Grenoble, France

*Correspondence to:* Arona DIEDHIOU (arona.diedhiou@ird.fr)

## Abstract.

The impact of initial soil moisture conditions on the mean climate over West Africa was examined using the latest version of the Regional Climate Model of the International Centre for Theoretical Physics (RegCM4) at a horizontal resolution of 25 km × 25 km. We performed these sensitivity studies on the initial conditions of soil moisture for June-July-August-September (JJAS) of two contrasted years 2003 (above normal precipitation year) and 2004 (below normal precipitation year). The soil moisture reanalysis of the European Centre Meteorological Weather Forecast's reanalysis of the 20th century (ERA20C) was used to initialize the control runs, whereas we initialized the soil moisture to the maximum and minimum value on our West African studied domain, corresponding to dry and wet initial soil moisture conditions respectively (hereafter dry and wet experiments). The impact of initial soil moisture condition on precipitation in West Africa is linear over the central and west Sahel where dry (wet) experiments lead to rainfall decrease (increase). The strongest precipitation increase is found over the West Sahel in wet experiments with a maximum change value of approximately +40%, while the strongest precipitation decrease is found in dry experiments over Central Sahel with a peak of change of approximately 4%. The sensitivity of anomalies in initial soil moisture condition can persist for three to four months (90-120 days) depending on the region. However, the influence on precipitation is no longer than one month (between 15 and 30 days). The strongest temperature decrease is located over the central and west Sahel with a maximum change of approximately -1.5 °C in wet experiments, while the strongest temperature increase is found over the Guinea coast and central Sahel in dry experiment with a maximum of change

around +0.6°C. A significant impact of initial soil moisture on the surface energy fluxes is observed in the wet (dry) experiments with a cooling (warming) of the surface temperature, an increase (decrease) sensible heat flux, a decrease (increase) of latent heat and an increase (decrease) of the boundary layer depth over the study area, with different magnitudes varying from one sub-region to another. Part II of this study investigates the influence of initial soil moisture initial conditions on climate extremes.

## 1 Introduction

In the climate system, soil moisture is a crucial variable that influence water balance and surface energy components through latent surface fluxes and evaporation. Therefore, soil moisture impacts the development of weather patterns and precipitation production. The strength of soil moisture impacts on land-atmosphere coupling varies according to location and season. Koster et al. (2004) sustained that the atmospheric response simulation to the slow variation of the ocean and land surface states, can improve seasonal simulations. The atmospheric response to ocean temperature anomalies has been well documented (Kirtman et al. 1998; Rasmusson et al.1982). Another potentially useful earth system component that varies slowly is soil moisture. Schär et al. (1999) sustained that the role of soils may be comparable to that of the oceans. The solar energy received by the oceans is stored in summer and used to heat the atmosphere in winter. The precipitation received by the soils is stored in winter and contributed to moisten and cool the atmosphere in summer. Through its impact on surface energy fluxes and evaporation, there are many additional impacts on the climate process of soil moisture, such as boundary-layer stability and air temperature (Hong and Pan, 2000; Kim and Hong 2006). Several studies have shown that the anomalies of soil moisture may persist for several weeks or months, however, its impact remains only for a shorter time in the atmosphere, not exceeding few days (Vinnikov and Yeserkepova 1991; Liu et al., 2014). One important role of anomalies in soil moisture in the coupling of land and atmosphere has been shown in several studies, using numerical climate models (Jaeger et al., 2011; Zhang et al., 2011) and observation datasets (Zhang et al., 2008a; Dirmeyer et al., 2006).

West Africa is known to exhibit strong coupling between soil moisture and precipitation (Koster et al., 2004). Several previous studies have been conducted over West Africa on a global scale using atmospheric general circulation model (AGCMs) to investigate the impact on the land-atmosphere coupling of soil moisture anomalies (Koster et al., 2004; Douville and al, 2001; Zhang et al., 2008b). However, at local and regional scales, the land-atmosphere coupling studies with AGCM, present significant uncertainties (Xue et al. 2010). Recently, RCMs have been used

to simulate the impact on interannual climate variability of anomalies in soil moisture which has received a lot of attention because of the increase in climate variability associated with extreme weather events that can have greater societal and environmental impacts. In general, these studies have been conducted in Asia, Europe and America (e.g. Seneviratne et al. 2006 for Europe; Zhang et al. 2011 for Asia; Zhang et al. 2008b for America). Overall, the results of these studies show that, during summer, the strong impact of the anomalies of soil moisture in land-atmosphere occurred mainly over the transition zones with a climate between wet and dry climate regimes. The relevance and extent of this potential feedback are still poorly understood in West Africa. This study will focus on the influence of initial soil moisture conditions anomalies on climate mean and it is based on performance assessment of the Regional Climate model version 4 coupled to the version 4.5 of the Community Land Model (RegCM4-CLM4.5) performed by Koné et al. (2018) where the ability of the model to reproduce the climate mean has been validated. This study aims to estimate the limits of the impact of internal forcing of initial soil moisture over West Africa region using a Regional Climate Model. Experiments carried out are sensitivity studies that give idealized results of the effect of the initial soil moisture. In this study (part I), the sensitivity of mean climate simulation to initial "wet" and "dry" soil moisture conditions is investigated. In part II of the article, the influence of initial soil moisture conditions on climate extremes will be explored. The descriptions of the model and experimental setup used in this study are presented in Section. 2; in the Section 3, the influence of the anomalies in soil moisture initial conditions on the subsequent climate mean is analyzed and discussed; and in Section 4 the main conclusions are presented.

## 2. Model and experimental design

### 2.1 Model description and observed datasets

The fourth generation of the Regional Climate Model (RegCM4) of the International Centre for Theoretical Physics (ICTP) was used in this study. Since its release, its physical representations have been continuously developed and implemented. The version used in the present study was RegCM4.7. The MM5 (Grell et al., 1994) non-hydrostatic dynamical core has been ported to RegCM without removing the existing hydrostatic core. The model dynamical core used in this study was non-hydrostatic. RegCM4 is a limited area model using a sigma pressure vertical grid and the finite differencing algorithm of Arakawa B-grid (Giorgi et al., 2012). The radiation scheme used in this version of RegCM4.7 is derived from the National Center for Atmospheric Research (NCAR) Community Climate Model Version three (CCM3) (Kiehl et al., 1996). Aerosols representation was taken from Zakey et al. (2006) and

Solmon et al. (2006). The large-scale precipitation scheme was taken from Pal et al. (2000) and the moisture scheme is the SUBgrid EXplicit moisture scheme (SUBEX). The SUBEX takes into account the sub-grid scale cloud variability, the accretion processes and evaporation for stable precipitation following the work of Sundqvist et al. (1989). In the planetary boundary layer (PBL), the sensible heat over ocean and land, water vapour and turbulent transport of momentum are calculated according to the scheme of Holtslag et al. (1990). Heat and moisture, the momentum fluxes of ocean surfaces in this study are computed as in Zeng et al. (1998). In RegCM4.7, convective precipitation and land surface processes can be described by several parameterizations. Based on Koné et al. (2018), we selected the convective scheme reported by Emanuel (1991) and the interaction processes between soil, vegetation and atmosphere are parameterized with CLM4.5. In each grid cell, CLM4.5 has 16 different Plant Functional Types (PFTs) and 10 soil layers (Lawrence et al., 2011; Wang et al., 2016). RegCM4 was integrated over the domain of West Africa depicted in Fig. 1 with 25 km (182x114 grid points; from 20° W-20° E and 5° S-21° N) with horizontal resolution and with 18 vertical levels and the initial and boundary conditions were taken from the European Centre for Medium-Range Weather Forecasts reanalysis (EIN75; Uppala et al., 2008; Simmons et al., 2007). The sea surface temperatures were obtained from the National Oceanic and Atmosphere Administration (NOAA) optimal interpolation weekly (OI_WK) (Reynolds et al., 1996). The topography data were taken from the States Geological Survey (USGS) Global Multi-resolution Terrain Elevation Data (GMTED; Danielson et al., 2011) at 30 arc-second spatial resolution, which is an update to the Global Land Cover Characterization (GTOPO; Loveland et al., 2000) dataset.

Our analysis focused on precipitation and the 2 m air temperature over the West African domain during the June-July-August-September (JJAS) summers in 2003 and 2004. Due to the coarse resolution of the climate observing network over the region, we validated the simulated precipitation based on two satellite derived products (Sylla et al., 2013a; Nikulin et al.,2012): the TRMM datasets (Tropical Rainfall Measuring Mission 3B43V7) at the high-resolution 0.25°, available from 1998 to 2013 (Huffman et al., 2007), and The Climate Hazards Group Infrared Precipitation with Stations (CHIRPS) dataset developed at the University of California at Santa Barbara at the 0.05° high-resolution available from 1981 to 2020. The validation of the simulated 2 m temperature relies on two observational datasets: the global daily temperature from the Global Telecommunication System (GTS), gridded at 0.5° of horizontal resolution for 1979 to 2020 (Fan and van den Dool, 2008) and the CRU datasets (Climate Research Unit version 3.20) from the University of East Anglia, gridded at a horizontal resolution of 0.5° for 1901 to 2011

(Harris et al., 2013). To facilitate comparison between RegCM4 simulations, all products were re-gridded to 0.22° × 0.22° using a bilinear interpolation method (Nikulin et al., 2012).

### 2.2 Experiments setup and analysis methodology

We designed an ensemble of three experiments, each with simulations starting from June 1st to September 30th. The difference between these three experiments is the change in the initial soil moisture condition during the first day of the simulation (June 1st). For each experiment, we applied a (i) reference initial soil moisture condition, (ii) wet initial soil moisture condition, and (iii) dry initial soil moisture condition.

We performed the simulations over 5 years (2001–2005) during the months of June to September over the West African domain. We selected two extreme years (wettest and driest year) over the study period to observe the estimates of the limits of the impact of internal soil moisture forcing on the new dynamical core non-hydrostatic of RegCM4. In the same context, several previous studies have selected two extreme years for their sensitivity study of initial soil moisture conditions on the models. Hong and al. (2000) used only two years (three months per year) to investigate the impact of initial soil moisture over North America (in the Great Plains) during two summers spanning May-June-July (MJJ) in 1988 (corresponding to a drought) and 1993 (corresponding to a flooding event). Kim and Hong (2006) selected two contrasting years 1997 (below normal precipitation) and 1998 (above normal precipitation year) for their study over east Asia. The first seven days (Kang et al., 2014) were excluded from the analysis as a spin-up period.

With very little variation in soil moisture in one day, initial soil moisture conditions are given in the first step of June 1 for JJAS 2003 and JJAS 2004. Except the geographical location, the experimental setup is the same as that of Hong and Pan (2000). The geographical location of this study is the same as in Koné et al. (2018), with four sub-regions (Fig. 1) exhibiting different features of the annual precipitation cycle: Central Sahel (10° W - 10° E; 10° N - 16° N), west Sahel (18° W - 10° W, 10° N - 16° N), and Guinea coast (15° W - 10° E; 3° N - 10° N). For each year, three experiments were conducted. We used the soil moisture from the reanalysis of the European Centre Meteorological Weather Forecast's reanalysis of the 20th century (ERA20C) to initialize the control runs. We initialized the dry and wet soil moisture initial conditions (in volumetric fraction $m^3.m^{-3}$) respectively at the minimum value ($=0.117*10^{-4}$) and the maximum value (=0.489) derived from ERA20C dataset over the West African studied domain.

In several previous studies (Liu et al., 2014; Hong and Pan, 2000; Kim and Hong, 2006), the mean biases (MB) averaged over their studied domains were used to quantify the impact of soil

moisture anomalies. In our study, we used the MB and probability density function (PDF; Gao et al., 2016; Jaeger and Seneviratne, 2011) by fitting a normal distribution to better capture how many grid points are impacted by initial soil moisture conditions. The pattern correlation coefficient (PCC) was also used as a spatial correlation to reveal the degree of large-scale similarity between model simulations and observations. We used two-tailed Student's t-distribution to investigate the differences that were statistically significant at each grid cell between the control and the sensitivity experiments (wet and dry). For the regional analysis such as MB, PCC, and the PDF, both modeled and observed temperature and precipitation values were calculated only over land grid points.

## 3. Results and discussion

### 3.1. Influence of initial soil moisture conditions on precipitation.

To identify the extreme years (driest and wettest) impacted by the dry and wet experiments among the simulation period (2001–2005), we determined changes in daily soil moisture and their climatological mean during JJAS over the West African domain from dry and wet experiments with respect to their corresponding control experiment. These changes are presented in Fig. 2, which shows that the weakest and strongest impacts of the dry experiments were observed in 2003 and 2004, respectively. In a wet year, the impact of soil drying is quickly erased. In a dry year, the impact of soil drying is accentuated. Thus, 2003 and 2004 are, respectively, the wettest and driest years in the dry experiment. However, for the wet experiments, the weakest impact was found for 2004, and the strongest impact was found for the years 2001, 2002, and 2004. In a dry year, the impact of soil humidification is very quickly mitigated, while in a wet year, the impact of soil humidification is accentuated. The wet experiments confirmed the results obtained in dry experiments, demonstrating that 2003 and 2004 are the wettest and driest years, respectively. From this analysis, 2003 and 2004 were selected to estimate the limits of the impact of internal soil moisture forcing on the new dynamical core non-hydrostatic of RegCM4. Figure 3 displays the spatial distribution of the observed mean rainfall (mm/day) from CHIRPS (Fig. 3a, d) and TRMM (Fig. 3b, e) for JJAS 2003 and JJAS 2004 and their corresponding simulated from control experiments (Fig. 3c, f) initialized with reanalysis soil moisture ERA20C. Table 1 reports the MB and PCC for model simulation and TRMM observation compared to CHIRPS, computed for the central Sahel, Guinea coast, west Sahel, and the entire West African domain. The CHIRPS product displays a zonal band of rainfall centered around 10° N, decreasing from north to south (Fig. 3a, d). The

maximum values are located over the mountain regions of Cameroun and Guinea. The TRMM observations (Fig. 3b, e) are closer to CHIRPS and are quite similar to the North–South gradient of precipitation with PCC up to 0.97 over the entire West African domain for both JJAS 2003 and JJAS 2004 (Table 1). However, although the observation datasets have similar large-scale patterns, they exhibit differences at the local scale. CHIRPS shows a much larger extent of these maxima than TRMM, especially over the Guinea highland and Cameroon mountains, while TRMM shows a large band of precipitation that extends too far into the Sahel region. The strongest MB between the two products are dry at approximately −15.45 % and −16.96 %, respectively, for JJAS 2003 and JJAS 2004 and are located over the Guinea coast sub-region (Table 1). The control experiments (Fig. 3 c and f) initialized with the reanalyzed ERA20C soil moisture effectively reproduced the large-scale pattern of observed rainfall with PCC 0.72 and 0.77 (Table 1), respectively, for JJAS 2003 and JJAS 2004 over the West Africa domain, despite some biases at the local scale. The spatial extent of rainfall maxima and the North–South gradient were well captured by control experiments; however, their magnitudes were underestimated. In general, dry MB of app −49.31% and −50.56% were obtained for JJAS 2003 and JJAS 2004 over the whole West African domain (Table 1). Fig. 4 displays the change in mean precipitation (in %) in JJAS 2003 and JJAS 2004 for dry and wet experiments with respect to their corresponding control experiments. The dotted area shows changes with a statistical significance of 0.05.

Dry and wet sensitivity experiments showed that precipitation was significantly affected by soil moisture anomalies at varying degrees according to the sub-regions (Fig. 4). For the dry experiments (Fig.4a, c), we found a dominant decrease in rainfall over the central Sahel especially in JJAS 2003 and JJAS 2004 (Fig.4a and c). On the other hand, we found a dominant increase in rainfall over the Guinea coast for both JJAS 2003 and JJAS 2004, and over the west Sahel particularly in JJAS 2003. For the wet experiments (Fig.4b, d), there is a dominant increase of rainfall over most of studied domains studied for both JJAS 2003 and JJAS 2004 (rep. Fig.4a and c). Overall, the impact of initial soil moisture conditions on the precipitation is linear only over the central Sahel for both JJAS 2003 and 2004 and somewhat over the west Sahel especially in JJAS 2004; that is, the dry (wet) experiments exhibits significant decrease (increase) in precipitations with respect to the control experiments (Fig.4a, b).

For a better quantitative evaluation, the PDF distributions of precipitation changes in JJAS 2003 and JJAS 2004, over (a) central Sahel, (b) west Sahel, (c) Guinea coast and (d) West Africa derived from dry and wet experiments compared to the corresponding control experiments are shown in Fig. 5. Table 3 summarizes the maximum values of changes obtained on the PDF's of

this study. The impact of initial soil moisture on precipitation was not linear over most of the studied domains (Fig.5 b-d) with the exception of central Sahel where the dry (wet) experiments display significant decrease (increase) in precipitation with respect to the control experiments (Fig.5a,). The strongest precipitation increase is found over west Sahel in wet experience in JJAS 2004, and the maximum change is about 40%. However, the strongest precipitation decrease is found over central Sahel in dry experiments in JJAS 2003 with a maximum change value reaching -4% (Table 3). The impacts on precipitation from wet experiments were greater than those from dry experiments (Table 3).

It is worth to note that, over the Guinea coast and the whole West African domain, for both dry and wet experiments cause an increase of precipitation (Fig. 5c and d). The dry year had a greater impact than the wet year in most of studied domains (Table 3). These results are consistent with previous studies that supported a strong relationship between precipitation and soil moisture in particular over the transition zones with a climate between wet and dry climate regimes (Koster et al., 2004; Liu et al., 2014; Douville et al., 2001).

To better study the influence of soil moisture anomalies on precipitation for both dry and wet years over the West African domain and its sub-regions, we analyzed changes in the daily domain-average of soil moisture and precipitation (Fig. 6 and Fig. 7, respectively) for JJAS 2003 and JJAS 2004, from dry and wet experiments with respect to their corresponding control experiments. The second soil layer in CLM4.5 (0 to 2.80 cm) corresponding to the top layer soil moisture was used in this study. In general, soil moisture anomalies persist for three or four months over the studied domains (Fig.6). Soil moisture anomalies disappeared for dry and wet experiments with varying durations, between three to four months from one region to another over the studied domain. The strongest duration and amplitude were found over the west Sahel sub-region, for both wet and dry experiments, it lasted for four months in JJAS 2003 and JJAS 2004, although the signal was rather weak in the wet experiments compared with the dry ones (Fig. 6b). A weaker change in soil moisture anomalies was found over the Guinea coast for wet experiments and lasted three months (Fig. 6c). In dry experiments, a weaker change in soil moisture anomalies was observed over central Sahel and lasted three months (Fig. 6a).

Figure 7 shows response of the daily precipitation to the initial soil moisture conditions over the different studied domain. In general, the impact of the wet soil moisture anomalies on daily precipitation is larger in magnitude than that of dry anomalies over most studied domains (Fig. 7). The strongest daily precipitation response in dry experiment (-4mm.day$^{-1}$) is found over the Guinea coast in the wet year JJAS 2003 (Fig. 7c), while for the wet experiments (more than 8mm.day$^{-1}$, especially in JJAS 2003), it was found over the west Sahel and the Guinea coast

(Fig. 7b and c, respectively). However, the impact of initial soil moisture conditions on daily precipitation is much shorter-lived than soil moisture change. A significant impact on daily precipitation, greater than 1mm.day$^{-1}$ is only shown in wet experiments, and did not last more than 15 days for most studied domains, except for the Guinea coast where it lasted approximately one month. It is worth to note the peaks in precipitation over west Sahel and Guinea coast (Fig. 7b and c, respectively) during August and September that coincide with fluctuation in the anomalies of soil moisture (Fig.6b and c). This indicates that soil moisture and precipitation feedback is strong during this period over the Guinea coast and west Sahel regions. The response of the daily precipitation to initial soil moisture conditions anomalies is also sensitive to wet and dry years. This is indicated by the lag between dry and wet experiments for JJAS 2003 and JJAS 2004 years (Fig. 7). The magnitude of impacts due to contrasting years is location dependent. For example, over Guinea coast, in the dry experiments, the wet year presents a greater impact compared to the dry year (Fig.7 c). A reversed trend was observed for central Sahel (Fig. 7a). These results are in line with previous works which argued that the soil moisture-atmosphere feedback strength and the land memory are place dependent (Vinnikov et al. 1996; Vinnikov and Yeserkepova 1991).

Fig. 8 and 9 show the vertical profile change in humidity and temperature for JJAS 2003 and JJAS 2004, respectively, from dry and wet experiments over the entire West Africa domain and its sub-region with respect to control experiments, as indicated in Fig. 1.

For the dry and wet experiments, the impact on humidity and temperature (Fig.8 and Fig.9) are significant in the lower troposphere. The dry (wet) soil moisture experiments in the lower and middle troposphere show drying (moistening) for humidity and warming (cooling) for temperature. This indicates that for dry (wet) experiments a weak (strong) dry convection over most of the studied domains (Fig.8 and Fig.9). The strongest impact on humidity and temperature in the lower and middle troposphere is found over central Sahel (Fig.8a and Fig. 9a). These results in the lower troposphere are consistent with the precipitation sensitivity, especially over the central Sahel in JJAS 2003 (Fig. 4a, b). However, over west Sahel and the Guinea coast this impact is somewhat low compared to that of central Sahel. In the dry experiments over the Guinea coast (Fig.8c), these trends are reversed above 500 hPa for humidity, indicating wet convection in this sub-region. These results in the lower atmosphere are consistent with the precipitation sensitivity over the Guinea coast (Fig.4a, c).

On the over hand, in the upper troposphere, the significant impact on humidity and temperature is found only for wet experiments, and exhibited a drying and warming respectively for humidity and temperature over most of studied domains (Fig.8 and Fig.9). In the wet experiments, the

impact on upper tropospheric variability of initial soil moisture conditions anomalies which was also reported by Hong and Pal (2000). The effect of soil moisture anomalies is mostly confined to the near-surface and somewhat in the upper troposphere. Furthermore, in the upper troposphere, relative humidity responses to initial soil moisture conditions anomalies are more sensitive at atmospheric temperature to the contrast of the year, especially, in wet experiments (Fig. 8 and Fig. 9).

To understand the causes of the precipitation changes illustrated in Fig. 4, we analyzed the lower tropospheric wind (850hpa) and moisture changes for JJAS 2003 and JJAS 2004 from the dry and wet experiments with respect to their corresponding control experiments; our findings are presented in Fig. 10. In the dry experiments, we observed a dominant decrease of moistening over most of studied domain; however, the strong wind magnitude change over the Atlantic Ocean increase moisture from the ocean to the Guinea coast and west Sahel. This can explain the increase precipitation over these sub-regions in the dry experiments. Over central Sahel, a weak change in wind magnitude was observed, leading to strong decrease in precipitation which is particularly notable in JJAS 2003 (Fig.4a). Conversely, for the wet experiments, an increase in moistening was observed over most of studied domain. The strong change in wind magnitude shifts the moistening from the north to the south, leading to increased precipitation over most of domain studied in wet experiments (Fig.4 b and d). These results are broadly consistent with the dry and wet precipitation changes shown in Figure 4.

Summarizing these results, the impact of initial soil moisture conditions anomalies was linear only over the central Sahel for both JJAS 2003 and 2004 and over the west Sahel, especially in JJAS 2004. The strongest precipitation decreasing (increasing) was observed over west Sahel (central Sahel) in dry (wet) experiment in JJAS 2003 (JJAS 2004) with maximum change reaching -4% (40%). The anomalies in initial soil moisture condition persist for three or four months, while the significant impact on precipitation, greater than 1mm.day$^{-1}$, of the anomalies in soil moisture is much shorter, no longer than one month. The anomalies in soil moisture initial conditions effect are mostly confined to the near-surface climate and somewhat in the upper troposphere.

### 3.2. Influence on temperature and other surface fluxes.

The spatial distribution of average temperature (°C) from CRU (Fig.11 a and d) and GTS (Fig.11 b and e) observations for JJAS 2003 and JJAS 2004 and their corresponding mean temperature simulated from control experiments (Fig.11 c and f) initialized with reanalysis soil moisture ERA20C are shown in Fig.10. Table 2 summarizes the PCC and MB between the simulation of

the temperatures and CRU observation, calculated for the west Sahel, central Sahel, Guinea coast and the entire West African domain.

The CRU temperature displays a zonal distribution over the whole West Africa domain. Maximum values of approximately 34 °C were observed over the Sahara, and the lowest temperatures were found on the Guinea coast especially in orographic regions such as Guinean highlands, Cameroon mountains and the Jos Plateau, where the temperature did not exceed 26°C. The two observation datasets GTS and CRU are similar at large spatial scale with PCC reaching 0.99 over the entire West African domain for both JJAS 2003 and JJAS 2004 (Table 2). However, the extension and the amplitude of these maxima and minima are quite different in the two sets of gridded observations. While GTS (Fig.11b and e) observation displays large (small) areas with maximum (minimum) values, CRU (Fig. 11a and d) presents small (large) area of these maxima (minima) values. The strongest mean warm biases between the two observation products, reaching 0.54°C and 0.67°C respectively for JJAS 2003 and JJAS 2004, are located over the west Sahel sub-region compared to the others sub-regions (Table 2). The control experiments (Fig.11 c and f) show good agreement in the representation of the large-scale pattern of the observed temperature (CRU) with PCC 0.99 for both JJAS 2003 and JJAS 2004 (Table 2), including the zone of the meridional gradient of the surface temperature between Sahara Desert and Guinea coast which is crucial for the African Easterly Jet evolution and formation (Thorncroft and Blackburn 1999; Cook 1999). However, some biases were noted at the local scale. The spatial extent of temperature maxima and minima are well reproduced by control experiments, however their magnitudes were overestimated. The strongest warm MB of control experiments with respect to CRU observation are approximately 2.68 °C and 2.14 °C respectively for JJAS 2003 and JJAS 2004, are found over the West Sahel sub-region (Table 2).

Fig. 12 shows changes in mean temperature (°C) for JJAS 2003 and JJAS 2004, from dry and wet experiments with respect to their corresponding control experiments. The dotted area shows changes that are statistically significant at the 0.05 level. In the dry experiments, for both JJAS 2003 and JJAS 2004, the dominant warm changes are located over most of area under the latitude 13° N, with maximum values located over the Guinea coast. On the other hand, for the wet experiments, we found a dominant cool change over the west and central Sahel.

For a better quantitative evaluation, the PDF distributions of the changes in mean temperature in JJAS 2003 and JJAS 2004, over (a) the central Sahel, (b) west Sahel, (c) Guinea and (d) West Africa derived from dry and wet experiments with respect to their corresponding control experiments are shown in Figure 13. The temperature impact is linear over the central Sahel, Guinea coast and the whole West African domain (Fig.13a, c and d). The strongest mean

368 temperature decrease was observe over the central and west Sahel (JJAS 2004 and JJAS 2003,
369 respectively; Table3) in wet experiences with the maximum change approximately -1.5 °C.
370 However, the strongest mean temperature increasing were found over the central Sahel (JJAS
371 2003) and the Guinea coast (JJAS 2004) in dry experiments reaching 0.56 °C and 0.59°C
372 respectively(Table 3). Overall, the dry (wet) sensitivity experiments for 2m-temperature showed
373 a dominant increase (decrease) in warming (cooling) for both JJAS 2003 and JJAS 2004 over
374 most of the studied domains, except for the west Sahel, where both dry and wet experiments lead
375 to an increase of temperature (Fig.13, Table3).
376 We now analyze the influence of initial soil moisture conditions anomalies on land energy
377 balance, particularly on the surface fluxes sensible and latent heat. Figure 14 shows changes in
378 sensible heat fluxes (in $W.m^{-2}$) for JJAS 2003 and JJAS 2004, from dry and wet experiments
379 compared to their corresponding control experiments, and the dotted area shows changes that are
380 statistically significant at the 0.05 level. As shown in figure 14, initial soil moisture conditions
381 anomalies strongly affect the sensible fluxes. The impact on sensible heat of initial soil moisture
382 condition anomalies was linear over most of the studied domains, that is, the dry (wet)
383 experiments with respect to the control exhibits significant increase (decrease) of the sensible
384 heat (Fig.14).
385 The PDF distributions of change in sensible heat flux are displayed in Figure 15. The dry (wet)
386 experiments show an increase (decrease) of the sensible flux in both JJAS 2003 and JJAS 2004
387 over studied domains (Fig. 15). The impact in wet experiments was strong compared to the dry
388 experiments over central and west Sahel except over Guinea coast (Fig. 15, Table 3). The
389 strongest increasing (decreasing) in sensible heat flux was found over Guinea coast (central
390 Sahel) in dry (wet) experiments, with maximum change about 9.18 $W.m^{-2}$ (-39.66 $W.m^{-2}$) in
391 JJAS 2004 (2003) (see Table 3).
392 Unlike the case of sensible heat flux, changes in latent heat show a linear opposite patterns, a
393 dominant decrease (increase) of latent heat flux is observed over most of studied domains in dry
394 (wet) experiment (Fig.16). The PDF distributions of latent heat flux change are shown in Figure
395 17. The results indicate that the impact on latent heat flux of soil moisture anomalies was linear,
396 that is, dry experiments result in a decrease in latent heat flux, while the wet experiments result
397 in an increase in the latent heat flux over most of studied domains. The strongest increase
398 (decrease) in latent heat flux was found in wet (dry) experiments over west Sahel (Guinea coast)
399 with maximum change reaching 36.49 $W.m^{-2}$ (-14.64$W.m^{-2}$) in JJAS 2004(Table3). It is worth to
400 note that the impacts on latent and sensible heat flux in wet experiments are strong compared to
401 the dry experiments over most of studied domains, except over Guinea coast (Table 3).

To determine whether most changes in energy go to evaporating water or to heating the environment, we analyzed the changes in Bowen ratio for JJAS 2003 and JJAS 2004, for dry and wet experiments with respect to their corresponding control experiments, the results are provided in Fig. 18. The dotted area displays statistically significant differences at the 0.05 level. The soil moisture anomalies strongly affected the Bowen ratio. The dry (wet) experiments show a dominant increase (decrease) of evaporation energy (Bowen ratio value in the range [0,1]) over most studied domains, except over the west Sahel for both JJAS 2003 and JJAS 2004 (Fig.18). As expected, the areas where most energy changes go to water evaporation are coincident with areas of temperature changes. The decrease (increase) in the evaporation area coincides with the decrease (increase) of temperature change.

For a quantitative evaluation, the PDF distribution of the Bowen ratio is shown in Figure 18. The impact of initial soil moisture conditions on the Bowen ratio was linear over most studied domain for both JJAS 2003 and JJAS 20004, except for west Sahel in JJAS 2003 (Fig. 18). The dry (wet) experiments show an increase (decrease) of water evaporation energy. The strongest increase (decrease) of energy going in evaporation is found over the central and west Sahel (over the central Sahel and Guinea coast) in JJAS 2004, in the dry (wet) experiments with maximum change reaching 0.39 and 0.41 (-0.64) respectively (Table 3). However, the strongest impact on energy going to heat the environment is found over the west Sahel reaching -3.01 and -2.41in dry and wet experiments respectively.

We then examine the impact on the stability of the PBL of the anomalies in initial soil moisture conditions. Soil moisture can influence rainfall by limiting evapotranspiration, which affects the development of the daytime PBL and thereby the initiation and intensity of convective precipitation (Eltahir, 1998). Fig. 20 shows changes in PBL (in m) for JJAS 2003 and JJAS 2004, from dry and wet experiments with respect to their corresponding control experiments with dotted areas that are statistically significant at the 0.05 level. The anomalies in initial soil moisture conditions impact significantly the PBL. The dry experiments demonstrated an dominant increase in PBL under the latitude 15° N for both JJAS 2003 and JJAS 2004 (Fig.20 a and c, respectively). For the wet experiments, a decrease in PBL is located over most of the studied domains. The PDF distribution of PBL changes, computed over the area indicated in Figure1 is shown in Fig. 21. The impact on PBL is linear over most of studied domains (Fig.21). The dry (wet) experiments lead to an increase (decrease) of PBL for both JJAS 2003 and JJAS 2004 over most of studied domains. The strongest increase (decrease) in PBL was found over Guinea coast (west Sahel) in dry (wet) experiments in JJAS 2004 (JJAS 2003) reaching 146.80m (293.23m). There is dry (wet) air above the area where there is increase (decrease) in PBL,

436 which results in warm (cool) and dry (moist) over most studied domains (see Fig. 8 and Fig. 9).
437 These results are consistent with the work of Han and Pan 2003.
438 Summarizing the results of this section, in the wet experiments, the cooling of mean surface
439 temperature is associated with a decrease of latent heat flux, an increase in sensible heat flux and
440 the PBL depth over most of the studied domain. Conversely, in the dry experiments, the
441 warming of surface temperature is associated with an increase of the latent heat flux, a decrease
442 of the sensible heat flux and PBL height. These results are consistent with those of Eltahir et al.
443 (1998). Furthermore, sensible and latent heat fluxes, Bowen ratio and PBL responses to initial
444 soil moisture conditions the anomalies are somewhat sensitive to the contrast of year and
445 experiments (wet and dry).
446

447 **4. Conclusion**
448 The impact of initial soil moisture conditions anomalies on the subsequent summer mean climate
449 over West Africa was explored using the RegCM4-CLM45. In particular, the aim of this study
450 was to investigate how soil moisture initialization at the beginning of the rainy season may affect
451 the intraseasonal variability of temperature and precipitation mean within the subsequent season
452 (June to September). For this purpose, three experiments each with simulations begining from
453 June 1st to September 30$^{th}$ were set up and runs were performed in JJAS 2003 and in JJAS 2004.
454 The difference between these 3 experiments is the change in initial soil moisture condition at the
455 beginning of the simulation: For each experiment, we applied a (i) control soil moisture initial
456 condition, (ii) wet soil moisture initial condition, and (iii) dry soil moisture initial condition.

457 The impact of initial soil moisture condition on precipitation depends on the location, magnitude
458 and persistence of initial soil moisture condition anomalies throughout the season. The impact of
459 initial soil moisture conditions anomalies was linear only over the central Sahel for both JJAS
460 2003 and 2004 over the west Sahel especially in JJAS 2004. The strongest precipitation decrease
461 (increase) is found over the central Sahel (over central Sahel) in dry (wet) experiment in JJAS
462 2003 (JJAS 2004) with maximum change reaching -4% (40%). Anomalies of initial soil
463 moisture condition can persist for three to four months (90-120 days) depending on the region of
464 West Africa but the impact on precipitation is no longer than 30 days (15 days over the Sahel
465 and 30 days over the Guinea Sahel).
466 Our results indicate that a wet soil moisture initial condition lead in the low levels of the
467 atmosphere to an increase of relative humidity associated with a cooling of temperature and in
468 the upper levels, to a decrease of relative humidity and a warming, while the dry experiment

mainly impact the lower levels with a decrease of the relative humidity associated with a warming. However, over the West Sahel and Guinea coast, the increase of precipitation shown in the dry experiments may result from the transport of moisture from the Atlantic Ocean by westerlies. The temperature is more sensitive to the anomalies of initial soil moisture condition than precipitation. The strongest impacts are located over the central Sahel with a maximum change of approximately -1.5 °C and 0.6°C respectively in wet and dry experiments. Our study showed significant impact of initial soil moisture conditions anomalies on the surface energy fluxes. We observed in wet (dry) experiments that the cooling (warming) of surface temperature was associated with an increase (decrease) of sensible heat flux, a decrease (increase) of latent heat and an increase (decrease) of the depth of the boundary layer over the region, with different magnitudes varying from one sub-region to another.

This study shows that soil moisture as a boundary condition plays a major role in controlling summer climate variability not only over the transition zone of climate but also, over humid zones such as Guinea coast. This study demonstrates that a good prescription of the initial condition of soil moisture can improve the simulation of precipitation and air temperature, which would help to reduce biases in climate model simulations. Overall, land surface initialization can contribute to improving sub-seasonal to seasonal forecast skill, but this requires further investigation. We recognize that sensitivity experiments such as "wet" and "dry" ones conducted in this study were not intended to simulate real climate since such extremes are very rare. These experiments, however, can facilitate estimation of the limits of internal forcing impact of soil moisture on the new non-hydrostatic dynamical core of RegCM4. Finally, in the context of climate change, considering the projected increase of high-impact weather events in the region, there is a need to explore the sensitivity of initial soil moisture conditions to climate extremes.

## Authors contributions

The authors declare to have no conflict of interest with this work. B. Koné and A. Diedhiou fixed the analysis framework. B. Koné carried out all the simulations and figures production according to the outline proposed by A. Diedhiou. Then B. Koné and A. Diedhiou, S. Anquetin and A. Diawara worked on the analyses. All authors contributed to the drafting of this manuscript.

## Acknowledgements

The research leading to this publication is co-funded by the NERC/DFID “Future Climate for Africa” programme under the AMMA-2050 project, grant number NE/M019969/1 and by IRD

(Institut de Recherche pour le Développement; France) grant number UMR IGE Imputation 252RA5.

**References:**

Beljaars A. C. M., Viterbo P. , Miller M. J., and Betts A. K.: The anomalous rainfall over the United States during July 1993: Sensitivity to land surface parameterization and soil moisture anomalies, Mon. Weather Rev., 124(3), 362–382, doi:10.1175/1520-0493(1996)124<0362: TAROTU>2.0.CO;2, 1996.

Bosilovich, M. G., and Sun W. Y.: Numerical simulations of the 1993 Midwestern flood: Land–atmosphere interactions. J. Climate, 12, 1490–1505, 1999.

Cook K. H.: Generation of the African easterly jet and its role in determining West African precipitation, J. Climate, 12, 1165–1184, https://doi.org/10.1175/1520-0442 (1999)012 <1165:GOTAEJ> 2.0.CO;2, 1999.

Danielson J.J., and Gesch D.B.: Global multi-resolution terrain elevation data 2010 (GMTED2010): U.S. Geological Survey Open-File Report 2011–1073, 26 p, 2011.

Dirmeyer P. A., Koster R. D., and Guo Z.: Do global models properly represent the feedback between land and atmosphere?, J. Hydrometeorol., 7(6), 1177–1198, doi:10.1175/JHM532.1, 2006.

Douville, F. Chauvin, and H. Broqua.: Influence of soil moisture on the Asian and African monsoons. Part I: Mean monsoon and daily precipitation. J. Climate, 14, 2381–2403, 2001.

Eltahir E. A. B.: A soil moisture-rainfall feedback mechanism 1. Theory and observations, Water Resour. Res., 34, 765–776, doi:10.1029/97WR03499, 1998.

Emanuel K. A.: A scheme for representing cumulus convection in large-scale models. Journal of the Atmospheric Science 48: 2313–2335, 1991.

Fan Y., and van den Dool H.: A global monthly land surface air temperature analysis for 1948 - present, J. Geophys. Res. 113, D01103, doi: 10.1029/2007JD008470, 2008.

Gao, X.-J., Shi, Y., and Giorgi, F.: Comparison of convective parameterizations in RegCM4 experiments over China with CLM as the land surface model, Atmos. Ocean. Sci. Lett., 9, 246–254, https://doi.org/10.1080/16742834.2016.1172938, 2016.

Giorgi F., Coppola E., Solmon F., Mariotti L., Sylla M. B., Bi X., Elguindi N., Diro G. T., Nair V., Giuliani G., Cozzini S., Guettler I., O'Brien T., Tawfik A., Shalaby A., Zakey A. S., Steiner A., Stordal F., Sloan L., and Brankovic C.: RegCM4: model description and preliminary tests over multiple CORDEX domains, Clim. Res., 52, 7–29, https://doi.org/10.3354/cr01018, 2012.

Grell G., Dudhia J. and Stauffer D. R.: A description of the fifth generation Penn State/NCAR Mesoscale Model (MM5), National Center for Atmospheric Research Tech Note NCAR/TN-398+STR, NCAR, Boulder, CO, 1994.

Harris I., Jones P. D., Osborn T. J. and Lister D. H.: Updated high-resolution grids of monthly climatic observations, Int. J. Climatol., 34, 623–642, https://doi.org/10.1002/joc.3711, 2013.

Holtslag A., De Bruijn E., and Pan H. L.: A high resolution air mass transformation model for short-range weather forecasting, Mon. Weather Rev., 118, 1561–1575, 1990.

Hong S-Y. and Pan H-L.: Impact of soil moisture anomalies on seasonal, summertime circulation over North America in a regional climate model. J. Geophys. Res., 105 (D24), 29 625–29 634, 2000.

Huffman G. J., Adler R. F., Bolvin D. T., Gu G., Nelkin E. J., Bowman K. P., Hong Y, Stocker E. F., and Wolff D. B.: The TRMM multisatellite precipitation analysis: quasi-global, multi-year, combined-sensor precipitation estimates at fine scale, J. Hydrometeorol., 8, 38-55, 2007.

Jaeger E. B., and Seneviratne S.I.: Impact of soil moisture-atmosphere coupling on European climate extremes and trends in a regional climate model, Clim. Dyn., 36(9-10), 1919-1939, doi:10.1007/s00382-010-0780-8, 2011.

Kang S, Im E.-S. and Ahn J.-B.: The impact of two land-surface schemes on the characteristics of summer precipitation over East Asia from the RegCM4 simulations Int. J. Climatol. 34: 3986-3997, 2014.

Kiehl J., Hack J., Bonan G., Boville B., Breigleb B., Williamson D., Rasch P. ; Description of the NCAR Community Climate Model (CCM3). National Center for Atmospheric Research Tech Note NCAR/TN-420+STR, NCAR, Boulder, CO, 1996.

Kim J-E., and Hong S-Y.: Impact of Soil Moisture Anomalies on Summer Rainfall over East Asia: A Regional Climate Model Study, Journal of Climate. Vol. 20, 5732–5743, DOI: 10.1175/2006JCLI1358.1, 2006.

Kirtman B.P., Schopf P. S.: Decadal Variability in ENSO Predictability and Prediction. Journal of Clim. 11, 2804, 1998.

Koné B., Diedhiou A., N'datchoh E. T., Sylla M. B., Giorgi F., Anquetin S., Bamba A., Diawara A., and Kobea A. T.: Sensitivity study of the regional climate model RegCM4 to different convective schemes over West Africa. Earth Syst. Dynam., 9, 1261–1278. https://doi.org/10.5194/esd-9-1261-2018, 2018.

Koster R. D., Dirmeyer P. A., Zhichang G., Bonan G., Chan E., Cox P., Gordon C. T., Kanae S., Kowalczyk E., Lawrence D., Liu P., Lu C. H, Malyshev S., McAvaney B., Mitchell K, Mocko D., Oki T., Oleson K., Pitman A., Sud Y. C. , Taylor C. M., Verseghy D., Vasic R., Xue Y., Yamada T.: Regions of strong coupling between soil moisture and precipitation, Science, 305, 1138–1140, doi:10.1126/science.1100217, 2004.

Lawrence D.M., Oleson K.W., Flanner M.G., Thornton P.E., Swenson S.C., Lawrence P.J. , Zeng X., Yang Z.-L., Levis S., Sakaguchi K., Bonan G.B., and Slater A.G.:Parameterization improvements and functional and structuraladvances in version 4 of the Community Land Model. J. Adv. Model. Earth Sys. 3. DOI:10.1029/2011MS000045, 2011.

600 Liu D., WangG. L., Mei R. , Yu Z. B. and Gu H. H.: Diagnosing the strength of land-atmosphere
601 coupling at sub-seasonal to seasonal time scales in Asia, J. Hydrometeor., doi:10.1175/JHM-D-
602 13-0104.1, 2013.
603
604 Liu D., G. Wang R. Mei Z. Yu, and Yu M.: Impact of soil moisture initial conditions anomalies
605 on climate mean and extremes over Asia, J. Geophys. Res. Atmos., 119, 529–545,
606 doi:10.1002/2013JD020890, 2014.
607
608 Loveland, T. R., Reed, B. C., Brown, J. F., Ohlen, D. O., Zhu, J., Yang, L., and Merchant, J. W.:
609 Development of a global land cover characteristics database and IGBP DISCover from 1-km
610 AVHRR Data, Int. J. Remote. Sens., 21, 1303–1330, 2000.
611
612 Oglesby R. J., and Erickson III D. J.: Soil moisture and the persistence of North American
613 drought. J. Climate, 2, 1362–1380, 1989.
614
615 Oglesby R. J., Marshall S. , Erickson III D. J., Roads J. O. and Robertson F. R.: Thresholds in
616 atmosphere-soil moisture interactions: Results from climate model studies. J. Geophys. Res.,107,
617 4244, doi:10.1029/2001JD001045, 2002.
618
619 Oleson K., Lawrence D. M., Bonan G. B., Drewniak B., Huang M., Koven C. D., Yang Z. -L.:
620 Technical description of version 4.5 of the Community Land Model (CLM) (No. NCAR/TN-
621 503+STR). doi:10.5065/D6RR1W7M, 2013.
622
623 Paeth H., Girmes R., Menz G. and Hense A.: Improving seasonal forecasting in the low latitudes,
624 Mon. Weather Rev., 134, 1859-1879, 2006.
625
626 Pal J. S., Small E. E. and Elthair E. A.: Simulation of regional scale water and energy budgets:
627 representation of subgrid cloud and precipitation processes within RegCM, J. Geophys. Res.,
628 105, 29579–29594, 2000.
629
630 Pal J. S. and Eltahir E. A. B.: Pathways relating soil moisture conditions to future summer
631 rainfall within a model of the land–atmosphere system. J. Climate, 14, 1227–1242, 2001.
632

633 Peterson T. C., Folland C., Gruza G., Hogg W. Mokssit A., Plummer N.: Report on the activities
634 of the working group on climate change detection and related rapporteurs 1998-2001. Geneva
635 (Switzerland): WMO Rep. WCDMP 47, WMO-TD 1071, 2001.
636
637 Nicholson S. E.: The West African Sahel: a review of recent studies on the rainfall regime and its
638 interannual variability, Meteorology, 453521, 32 p., https://doi.org/10.1155/2013/453521, 2013.
639 Nikulin G., Jones C., Samuelsson P., Giorgi F., Asrar G., Büchner M., Cerezo-Mota R.,
640 Christensen O. B., Déque M., Fernandez J., Hansler A., van Meijgaard E., Sylla M. B. and
641 Sushama L.: Precipitation climatology in an ensemble of CORDEX-Africa regional climate
642 simulations, J. Climate, 6057–6078, https://doi.org/10.1175/JCLI-D-11-00375.1, 2012.
643
644 Rasmusson E. M. and Carpenter T. H.: Variations in Tropical Sea Surface Temperature and
645 Surface Wind Fields Associated with the Southern Oscillation/El Niño. Mon. Weather Rev. 110,
646 354, 1982.
647
648 Reynolds, R. W. and Smith, T. M.: Improved global sea surface temperature analysis using
649 optimum interpolation, J. Climate, 7, 929–948, 1994.
650
651 Seager R., and Vecchi G. A.: Greenhouse warming and the 21st century hydroclimate of
652 southwestern North America. Proc. Natl. Acad. Sci. USA, 107, 21 277–21 282,
653 doi:10.1073/pnas.0910856107, 2010.
654
655 Simmons A. S., Uppala D. D. and Kobayashi S.: ERA-interim: new ECMWF reanalysis products
656 from 1989 onwards, ECMWF Newsl., 110, 29–35, 2007.
657
658 Solmon F., Giorgi F., and Liousse C.: Aerosol modeling for regional climate studies: application
659 to anthropogenic particles and evaluation over a European/African domain, Tellus B, 58, 51–72,
660 2006.
661
662 Sundqvist H. E., Berge E., and Kristjansson J. E.: The effects of domain choice on summer
663 precipitation simulation and sensitivity in a regional climate model, J. Climate, 11, 2698-2712,
664 1989.

Thorncroft, C. D. and Blackburn, M.: Maintenance of the African easterly jet, Q. J. R. Meteorol Soc., 125, 763–786, 1999.

Uppala S., Dee D., Kobayashi S., Berrisford P. and Simmons A.: Towards a climate data assimilation system: status update of ERA-interim, ECMWF Newsl., 15, 12–18, 2008.

Vinnikov K. Y. and Yeserkepova I. B.: Soil moisture: Empirical data and model results, J. Clim., 4(1), 66–79, doi:10.1175/1520-0442(1991) 004<0066:SMEDAM>2.0.CO;2, 1991.

Vinnikov K. Y., Robock A., Speranskaya N. A. and Schlosser A.: Scales of temporal and spatial variability of midlatitude soil moisture, J. Geophys. Res., 101(D3), 7163–7174, doi:10.1029/95JD02753, 1996.

Wang, G., Yu, M., Pal, J. S., Mei, R., Bonan, G. B., Levis, S., and Thornton, P. E.: On the development of a coupled regional climate vegetation model RCM-CLM-CN-DV and its validation its tropical Africa, Clim. Dynam, 46, 515–539, 2016.

Xue Y., De Sales F., Lau K. M. W., Bonne A., Feng J., Dirmeyer P., Guo Z., Kim K. M., Kitoh A., Kumar V., Poccard-Leclercq I., Mahowald N., Moufouma-Okia W., Pegion P., Rowell D. P., Schemm J., Schulbert S., Sealy A., Thiaw W. M., Vintzileos A., Williams S. F. and Wu M. L.: Intercomparison of West African Monsoon and its variability in the West African Monsoon Modelling Evaluation Project (WAMME) first model Intercomparison experiment, Clim. Dynam., 35, 3–27, https://doi.org/10.1007/s00382-010-0778-2, 2010.

Zakey A. S., Solmon F., and Giorgi F.: Implementation and testing of a desert dust module in a regional climate model, Atmos. Chem. Phys., 6, 4687–4704, https://doi.org/10.5194/acp-6-4687-2006, 2006.

Zeng X., Zhao M. and Dickinson R .E.: Intercomparison of bulk aerodynamic algorithms for the computation of sea surface fluxes using TOGA COARE and TAO DATA, J. Climate, 11, 2628-2644, 1998.

Zhang, J., W.-C. Wang, and J. Wei, Assessing land-atmosphere coupling using soil moisture from the Global Land Data Assimilation System and observational precipitation, J. Geophys. Res., 113, D17119, doi:10.1029/2008JD009807, 2008.

Zhang, J., W.-C. Wang, and L. R. Leung.: Contribution of land-atmosphere coupling to summer climate variability over the contiguous United States, J. Geophys. Res., 113, D22109, doi:10.1029/2008JD010136, 2008.

Zhang, J. Y., L. Y. Wu, and W. Dong,: Land-atmosphere coupling and summer climate variability over East Asia, J. Geophys. Res., 116, D05117, doi 10.1029/2010JD014714, 2011.

**Tables and figures:**

| | Central Sahel | | West Sahel | | Guinea | | West Africa | |
|---|---|---|---|---|---|---|---|---|
| | **PCC** | **MB (%)** | **PCC** | **MB (%)** | **PCC** | **MB (%)** | **PCC** | **MB (%)** |
| **TRMM 2003** | **0.98** | **7.60** | **0.96** | **-945** | **0.98** | **-15.45** | **0.97** | **-0.57** |
| **CTRL_2003** | **0.98** | **-47.97** | **0.87** | **-75.76** | **0.82** | **-47.12** | **0.73** | **-49.31** |
| **TMM 2004** | **0.98** | **-0.62** | **0.99** | **-7.03** | **0.98** | **-16.96** | **0.97** | **-1.56** |
| **CTRL_2004** | **0.98** | **-47.89** | **0.87** | **-68.35** | **0.85** | **-51.97** | **0.77** | **-50.56** |

**Table1:** The pattern correlation coefficient (PCC) and the mean bias (MB) for JJAS precipitation for model simulation and observation TRMM with respect to CHIRPS, calculated for Guinea coast, central Sahel, west Sahel and the entire West African domain during the period 2003 and 2004.

| | Central Sahel | | West Sahel | | Guinea | | West Africa | |
|---|---|---|---|---|---|---|---|---|
| | **PCC** | **MB (°C)** | **PCC** | **MB (°C)** | **PCC** | **MB (°C)** | **PCC** | **MB (°C)** |
| **GTS 2003** | **0.99** | **0.31** | **0.99** | **0.54** | **0.99** | **0.28** | **0.99** | **0.39** |
| **CTRL_2003** | **0.99** | **1.52** | **0.99** | **2.68** | **0.99** | **-0.34** | **0.99** | **0.85** |
| **GTS 2004** | **0.99** | **0.32** | **0.99** | **0.67** | **0.99** | **0.28** | **0.99** | **0.40** |
| **CTRL_2004** | **0.99** | **1.50** | **0.99** | **2.14** | **0.99** | **-0.57** | **0.99** | **0.51** |

**Table2:** The pattern correlation coefficient (PCC) and the mean bias (MB) for JJAS 2m-temperature for model simulation and observation (GTS) with respect to CRU, calculated for Guinea coast, central Sahel, west Sahel and the entire West African domain during the period 2003 and 2004.

| | | Central Sahel | | West Sahel | | Guinea coast | | West Africa | |
|---|---|---|---|---|---|---|---|---|---|
| | | ΔWC | ΔDC | ΔWC | ΔDC | ΔWC | ΔDC | ΔWC | ΔDC |
| Precipitation (%) | 2003 | 13.80 | **-4.09** | 29.95 | 6.58 | 19.40 | 9.20 | 8.88 | 4.68 |
| | 2004 | 15.86 | -3.29 | **38.58** | -1.25 | 26.6 | 12.68 | 10.72 | 7.64 |
| Temperature mean (°C) | 2003 | -1.48 | **0.56** | **-1.55** | -0.41 | -0.15 | 0.54 | -0.62 | 0.50 |
| | 2004 | **-1.51** | 0.47 | -1.15 | -0.24 | -0.19 | **0.59** | -0.41 | 0.59 |
| Sensible heat ($w.m^{-2}$) | 2003 | -16.89 | 8.57 | **-39.66** | 5.31 | -2.41 | 7.52 | -14.32 | 8.06 |
| | 2004 | -19.53 | 7.55 | -31.97 | 7.23 | -3.01 | **9.18** | -14.46 | 6.81 |
| Latent heat ($w.m^{-2}$) | 2003 | 21.27 | -6.67 | 34.21 | -6.06 | 3.09 | -13.38 | 15.86 | -8.07 |
| | 2004 | 28.55 | -4.81 | **36.49** | -6.20 | 7.09 | **-14.64** | 19.68 | -8.53 |
| Bowen ratio | 2003 | -0.42 | 0.31 | **-3.01** | -0.05 | -0.03 | 0.12 | -0.48 | 0.28 |
| | 2004 | **-0.64** | **0.39** | -2.49 | **0.41** | **-0.64** | 0.15 | -0.57 | 0.26 |
| PBL | 2003 | -233.49 | 81.23 | **-293.23** | -0.16 | -94.42 | 132.74 | -128.90 | 75.57 |
| | 2004 | -223.06 | 49.48 | -247.08 | 19.87 | -119.38 | **146.80** | -117.69 | 56.53 |

**Table3:** Table summarizing the maximum values of change obtained on the PDF distribution for precipitation, temperature, sensible heat, latent heat, Bowen ratio and PBL, calculated for Guinea coast, central Sahel, west Sahel and the entire West African domain during the period 2003 and 2004.

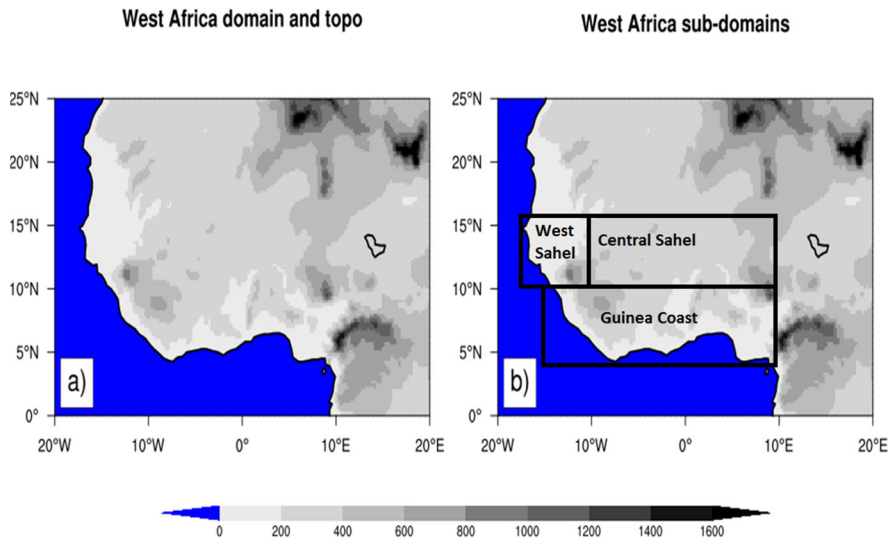


**Figure 1:** Topography of the West African domain. The analysis of the model result has an emphasis on the whole West African domain and the three subregions Guinea coast, central Sahel and west Sahel, which are marked with black boxes.

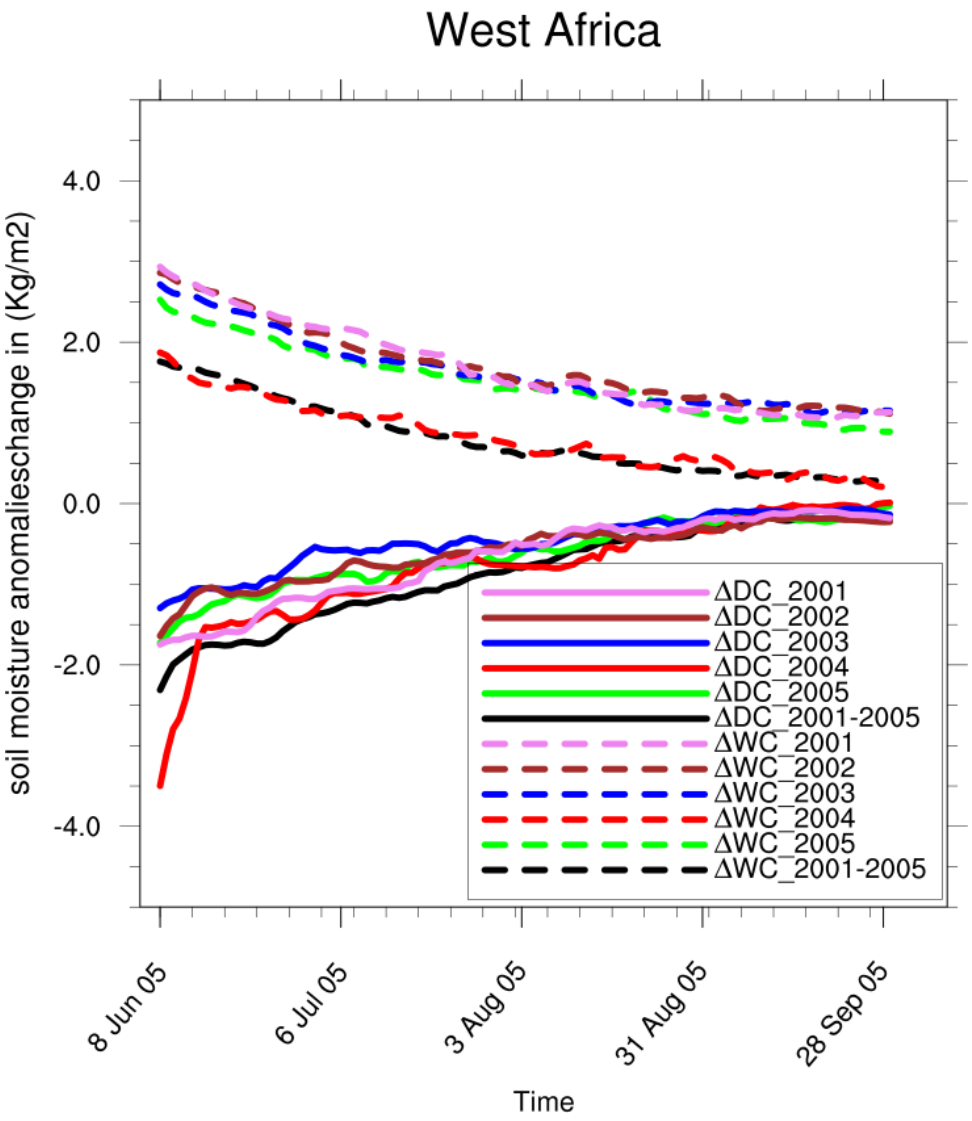


**Figure 2:** Changes in daily soil moisture for 5 years (2001 to 2005) and their climatological mean during JJAS over West African domain, from dry (ΔDC) and wet (ΔWC) experiments with respect to their corresponding control experiment.

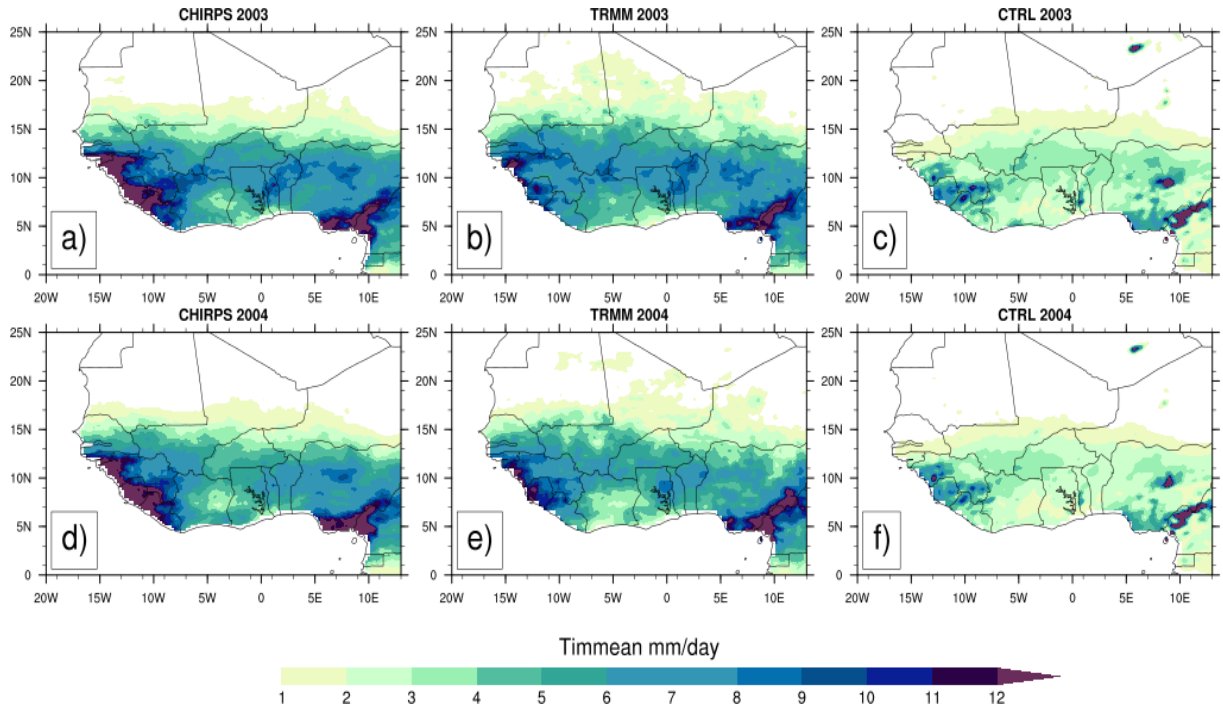


**Figure3:** Observed 4-month averaged (JJAS) precipitation (mm/day) from CHIRPS (a and d) and TRMM (b and e) for 2003 and 2004 and their corresponding mean rainfall simulated control experiments (CTRL) (c and f) with the reanalysis initial soil moisture ERA20C.

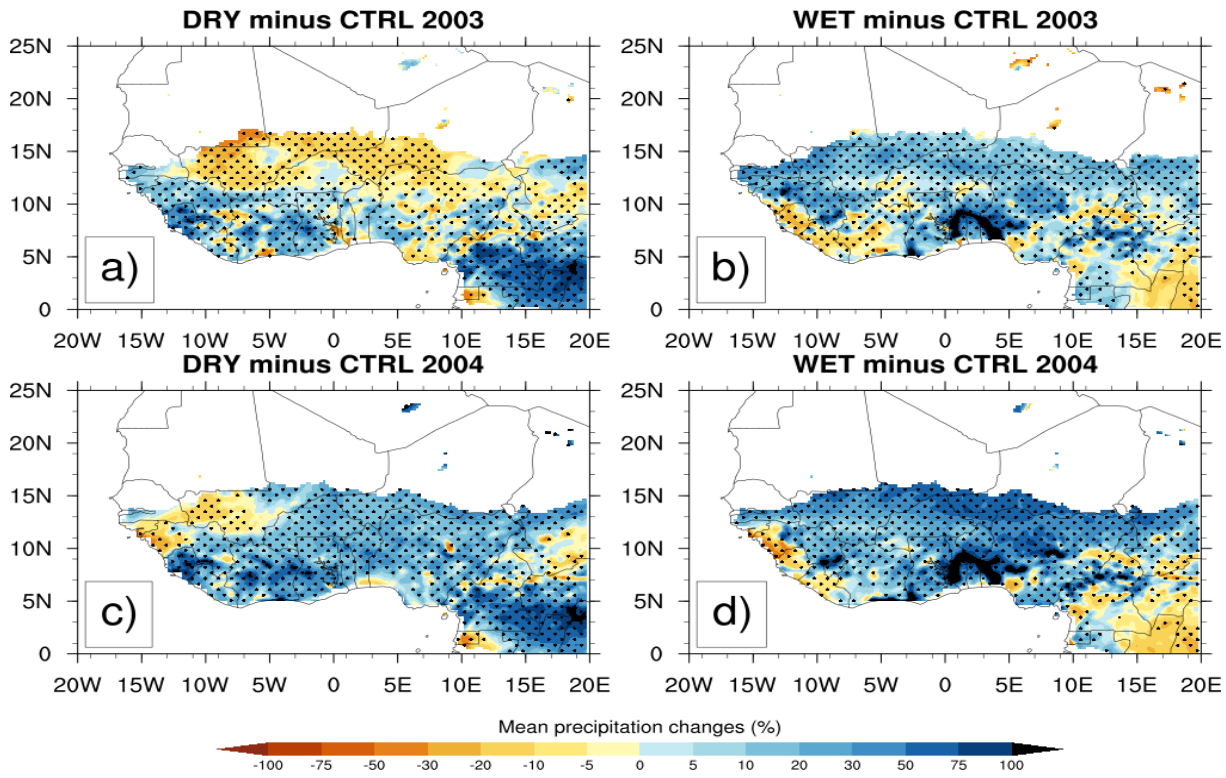


**Figure4:** Changes in mean precipitation (in %) for JJAS 2003 and JJAS 2004, from dry (resp. a and c) and wet (resp. b and d) experiments with respect to their corresponding control experiment, the dotted area shows differences that are statistically significant at 0.05 level.

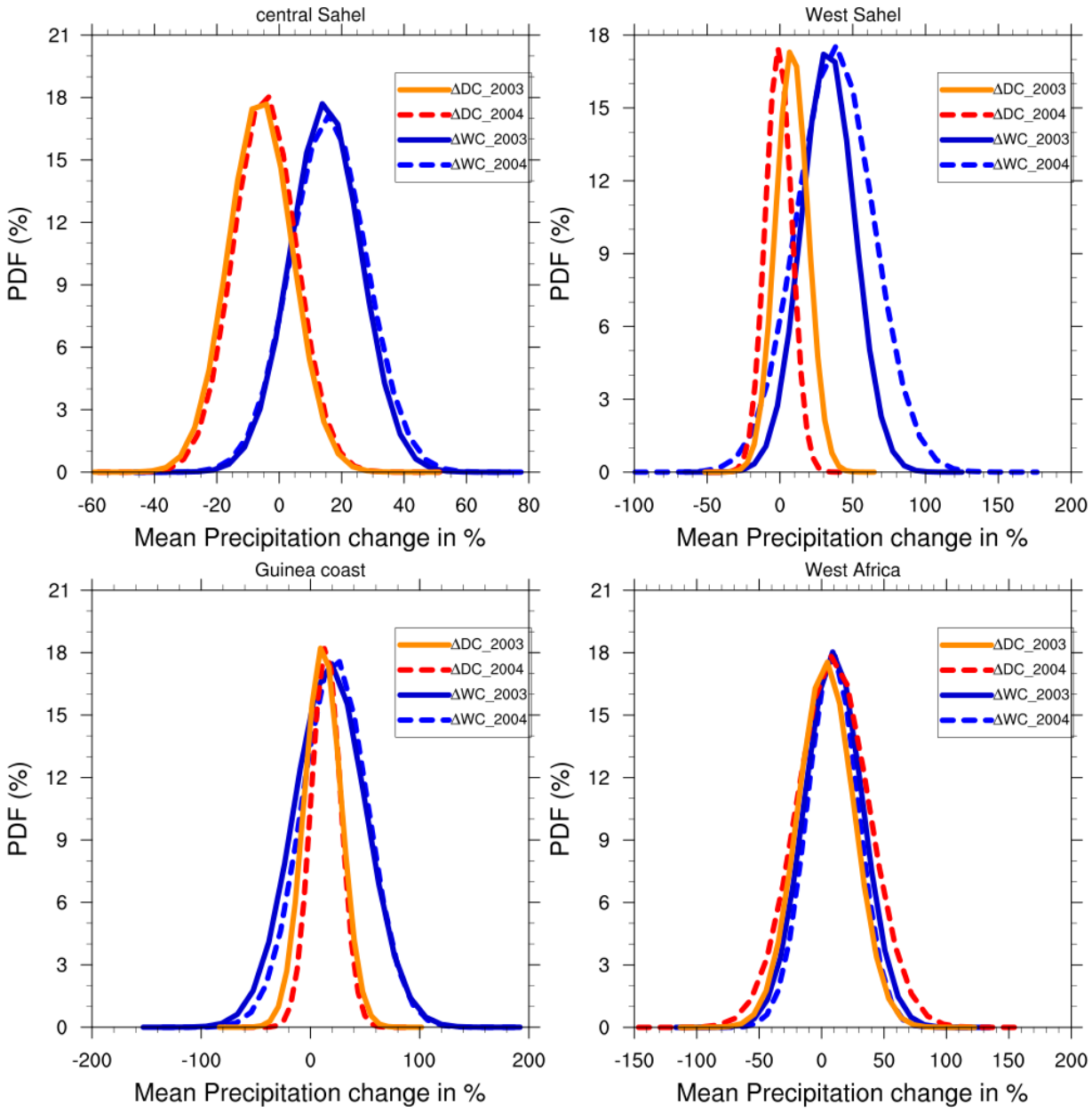


**Figure 5:** PDF distributions (%) of mean precipitation changes in JJAS 2003 and JJAS 2004, over (a) central Sahel, (b) West Sahel, (c) Guinea and (d) West Africa derived from dry (ΔDC) and wet (ΔWC) experiments compared to their corresponding control experiment.

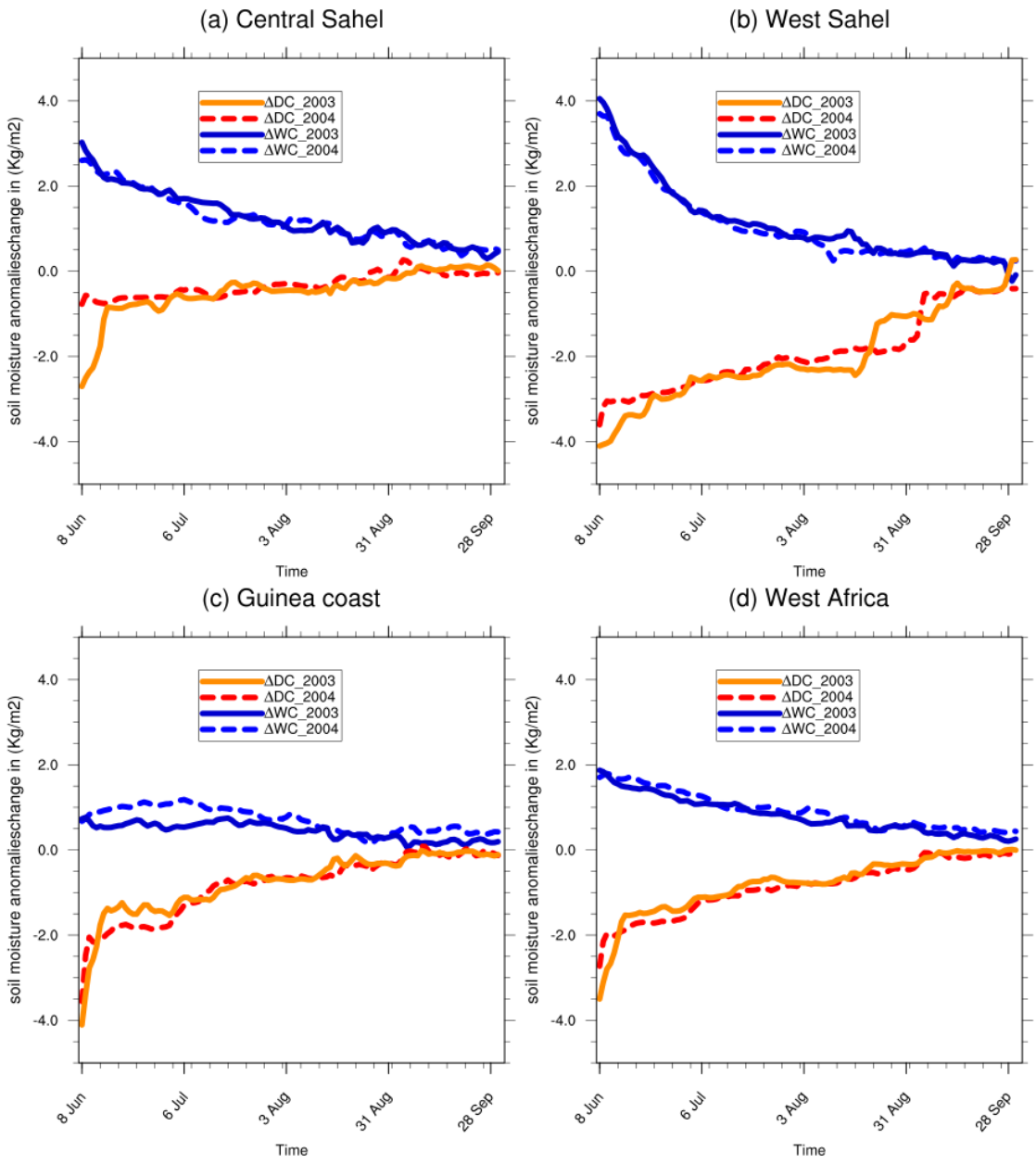


**Figure 6:** Daily domain-average soil moisture changes for JJAS 2003 and JJAS 2004, from dry (ΔDC) and wet (ΔWC) experiments with respect to their corresponding control experiment.

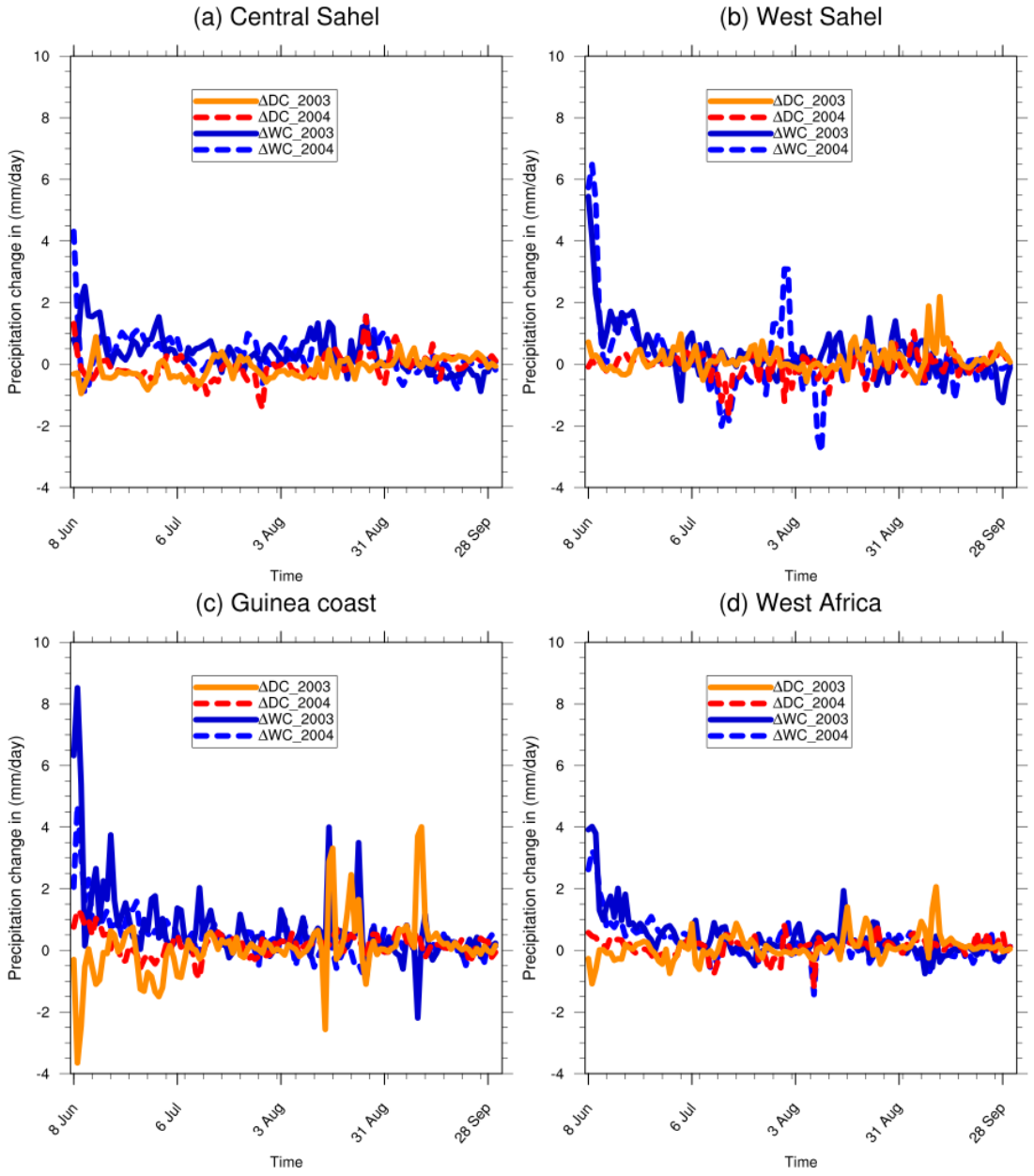


878
879
880

881 **Figure 7:** Daily domain-average precipitation changes for JJAS 2003 and JJAS 2004, from dry
882 (ΔDC) and wet (ΔWC) experiments with respect to their corresponding control experiment.

883
884
885
886
887
888
889

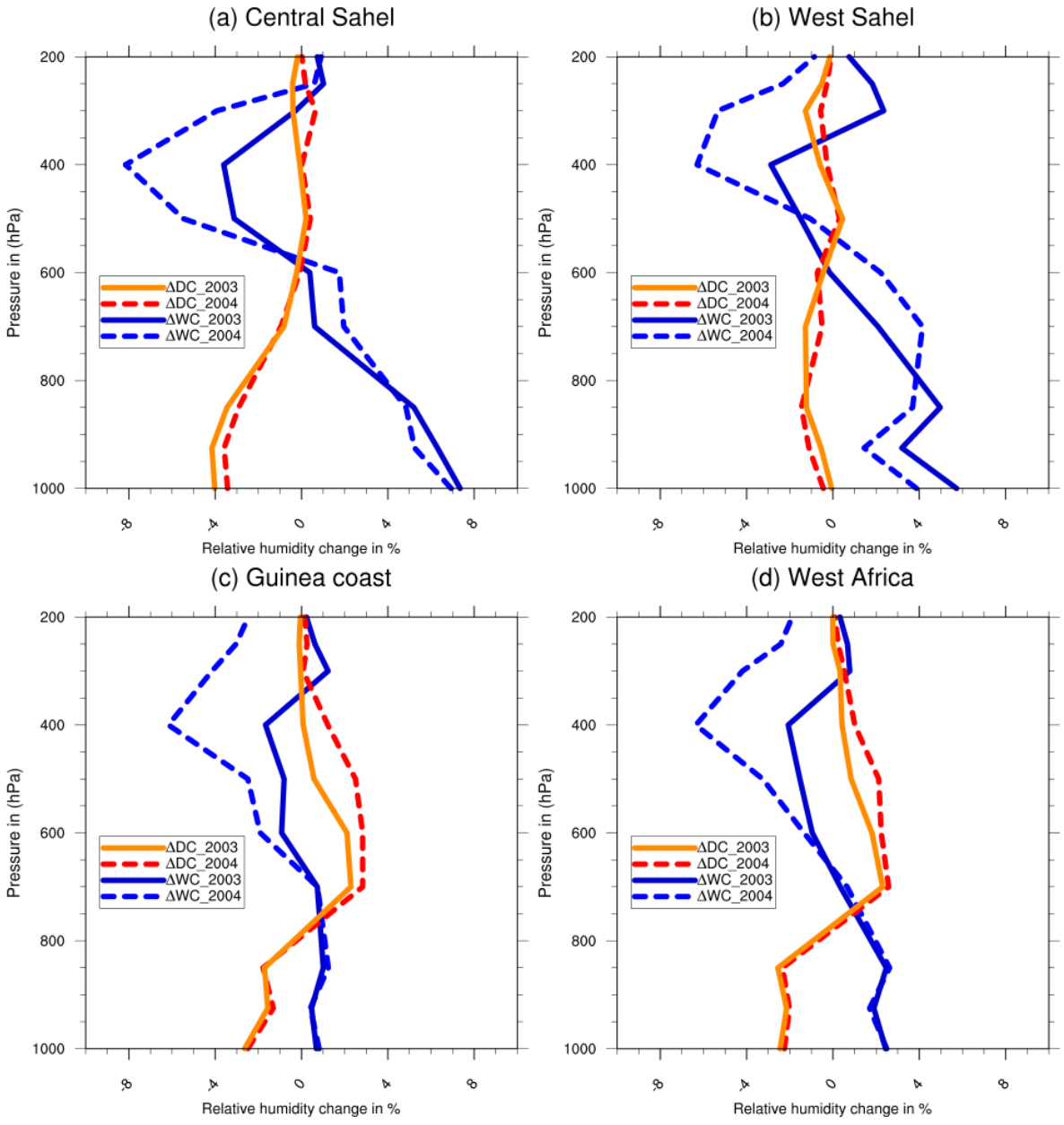


**Figure 8:** Vertical profile changes in Relative humidity for JJAS 2003 and JJAS 2004 from the dry (ΔDC) and wet (ΔWC) experiments with respect to corresponding control experiment over (a) central Sahel, (b) west Sahel, (c) Guinea coast, and (d) West Africa.

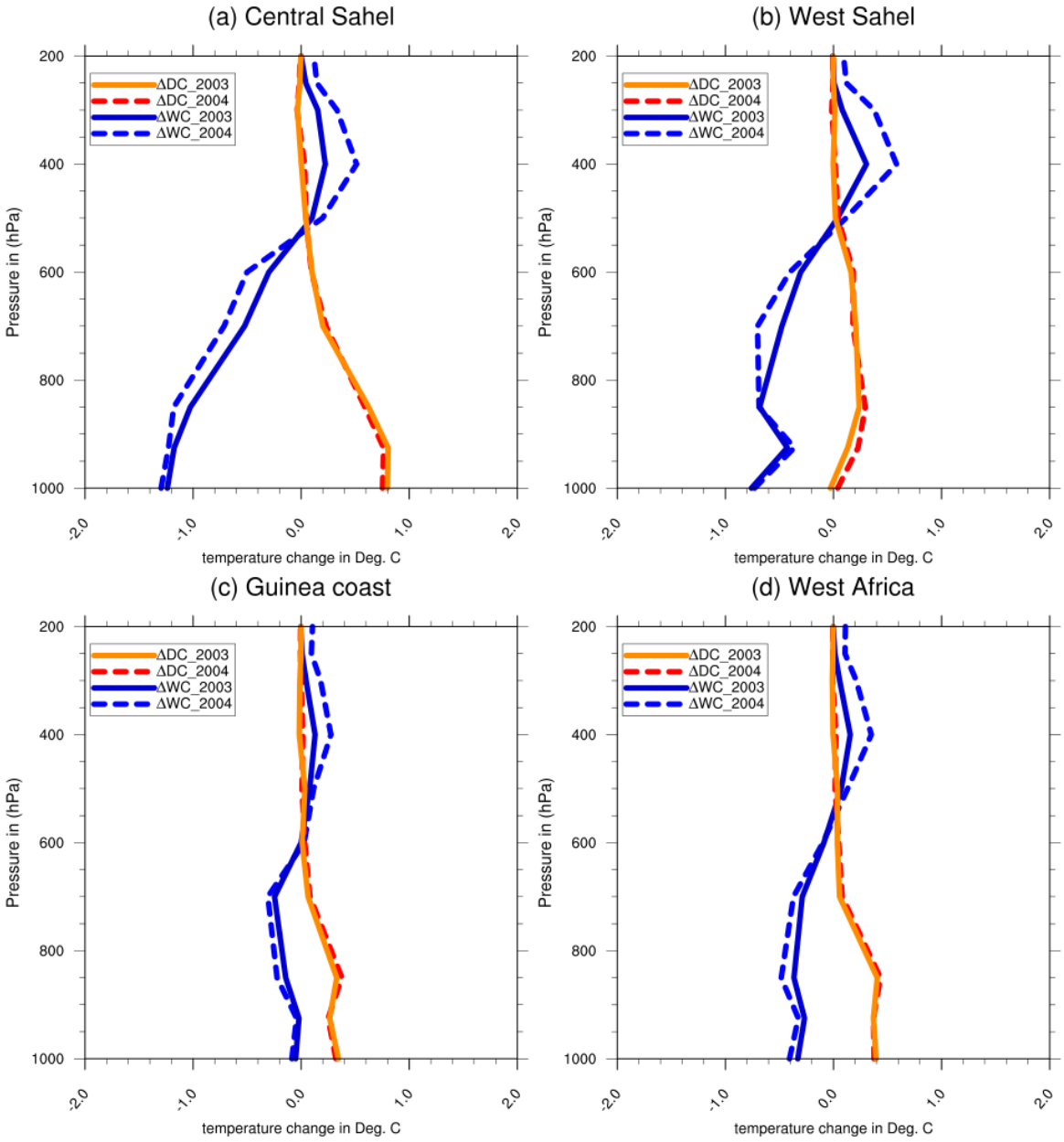


**Figure 9:** Vertical profile changes in temperature for JJAS 2003 and JJAS 2004 from the dry (ΔDC) and wet (ΔWC) experiments with respect to their corresponding control experiment over (a) central Sahel, (b) west Sahel, (c) Guinea coast, and (d) West Africa.

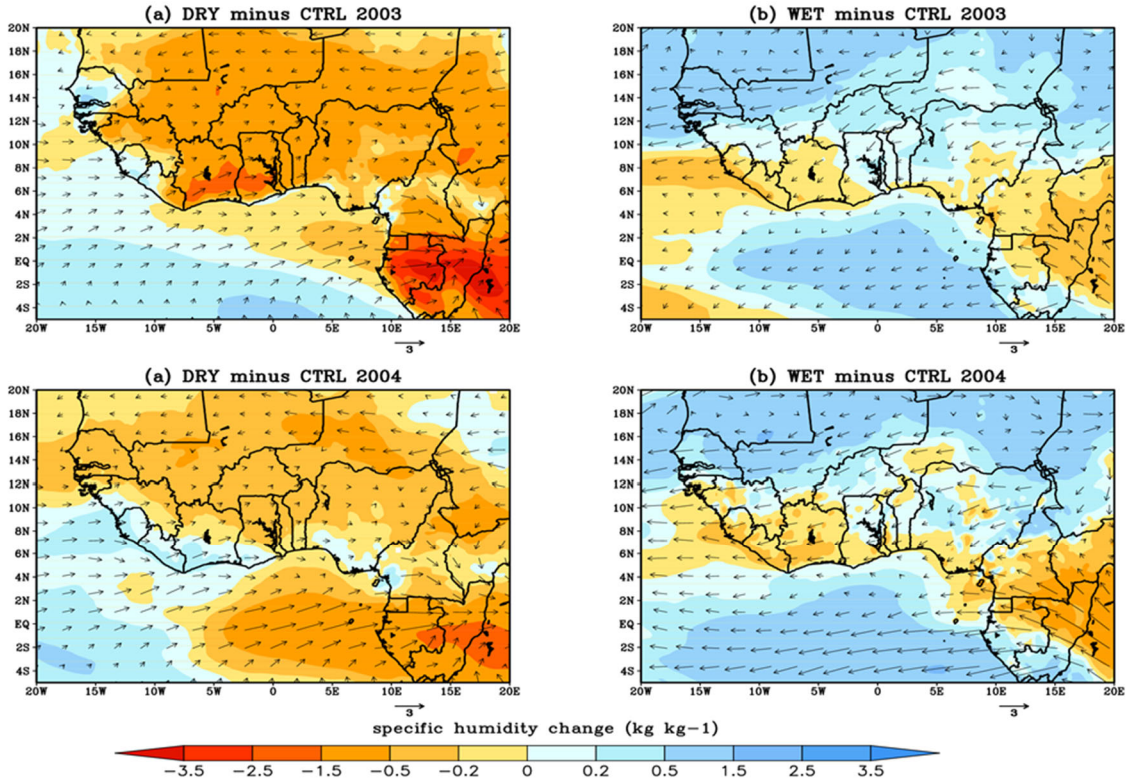


**Figure 10:** The lower tropospheric wind (850hpa) and moisture bias for JJAS 2003 and JJAS 2004 from the dry (a and c) and wet (b and d) experiments with respect to their corresponding control experiment.

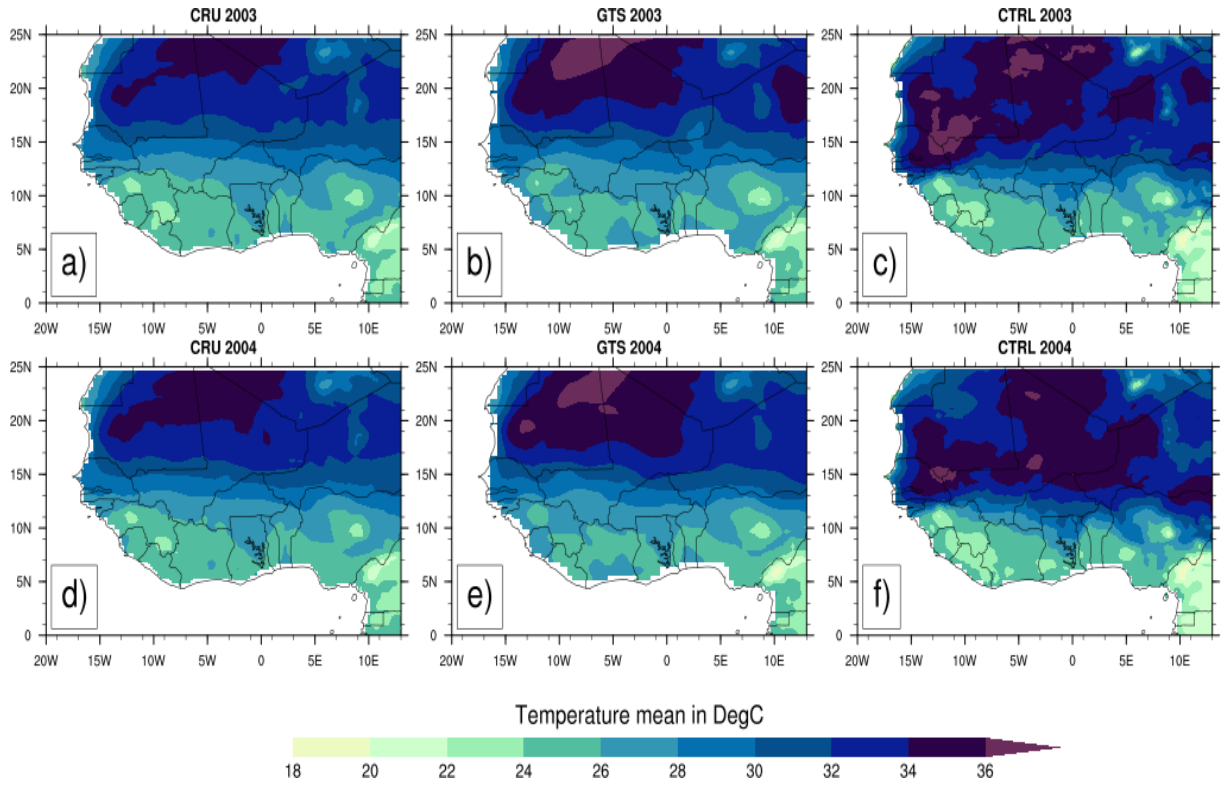


**Figure 11:** Observed 4-month averaged (JJAS) 2m-temperature (°C) from CRU (a and d) and GTS (b and e) for 2003 and 2004 and their corresponding mean temperature simulated control experiment (c and f) with the reanalysis initial soil moisture ERA20C.

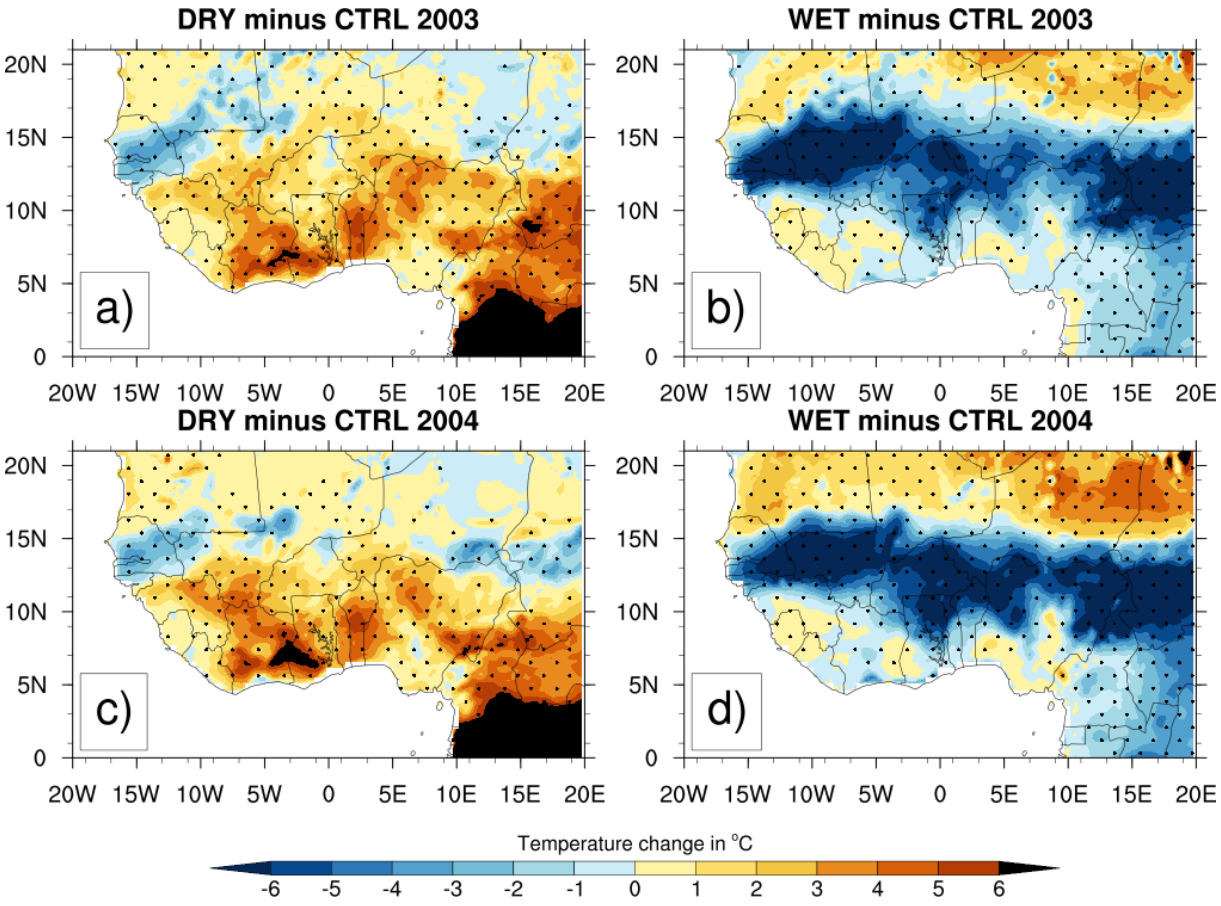


**Figure 12:** Changes in 2m-temperature (°C) for JJAS 2003 and JJAS 2004, from dry (resp. a and c) and wet (resp. b and d) experiments with respect to their corresponding control experiment, the dotted area shows differences that are statistically significant at 0.05 level.

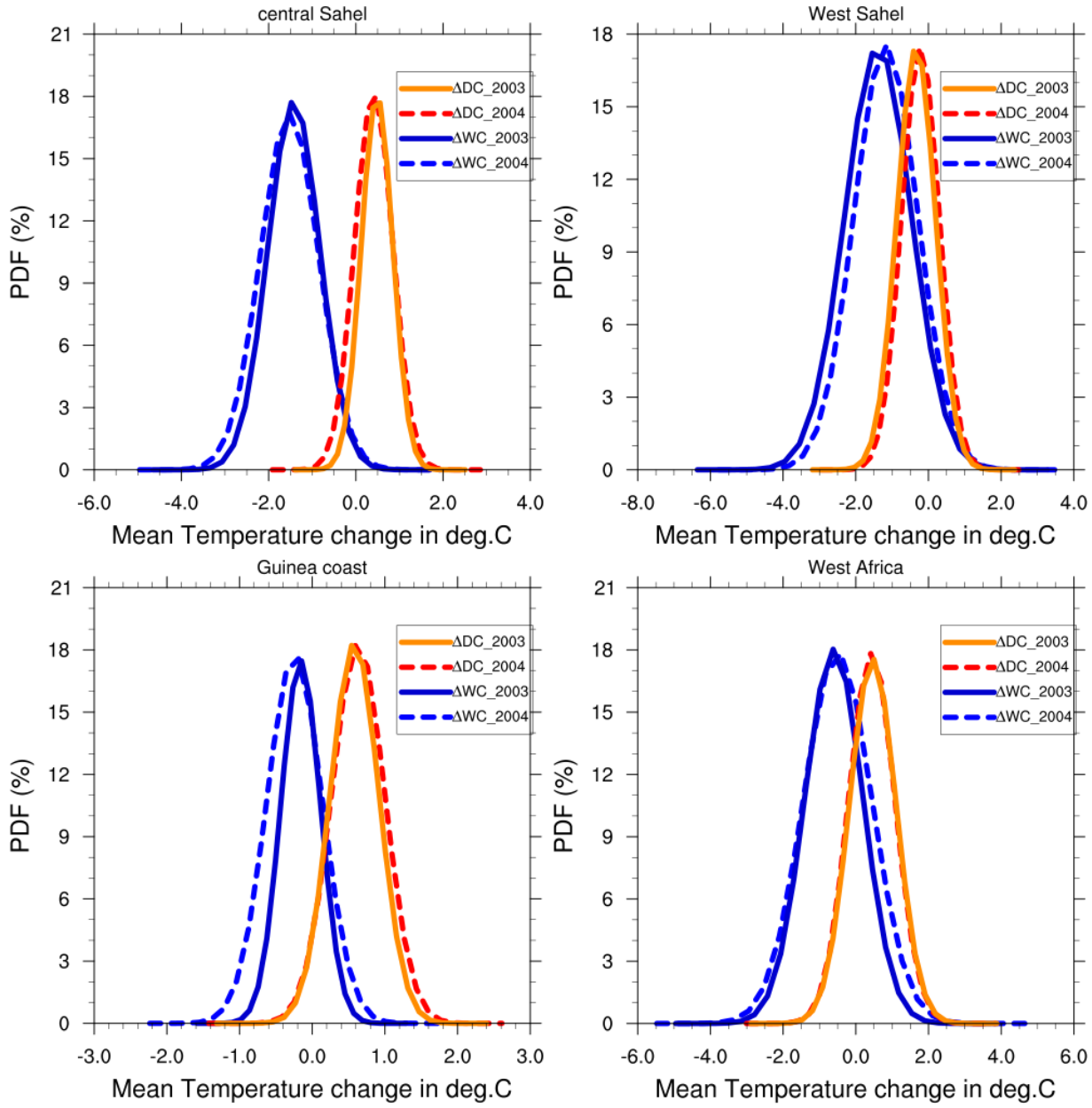


965
966

967 **Figure 13:** PDF distributions (%) of mean temperature changes in JJAS 2003 and JJAS 2004,
968 over (a) central Sahel , (b) West Sahel, (c) Guinea and (d) West Africa derived from dry (ΔDC)
969 and wet (ΔWC) experiments compared to their corresponding control experiment.

970
971
972
973
974
975
976

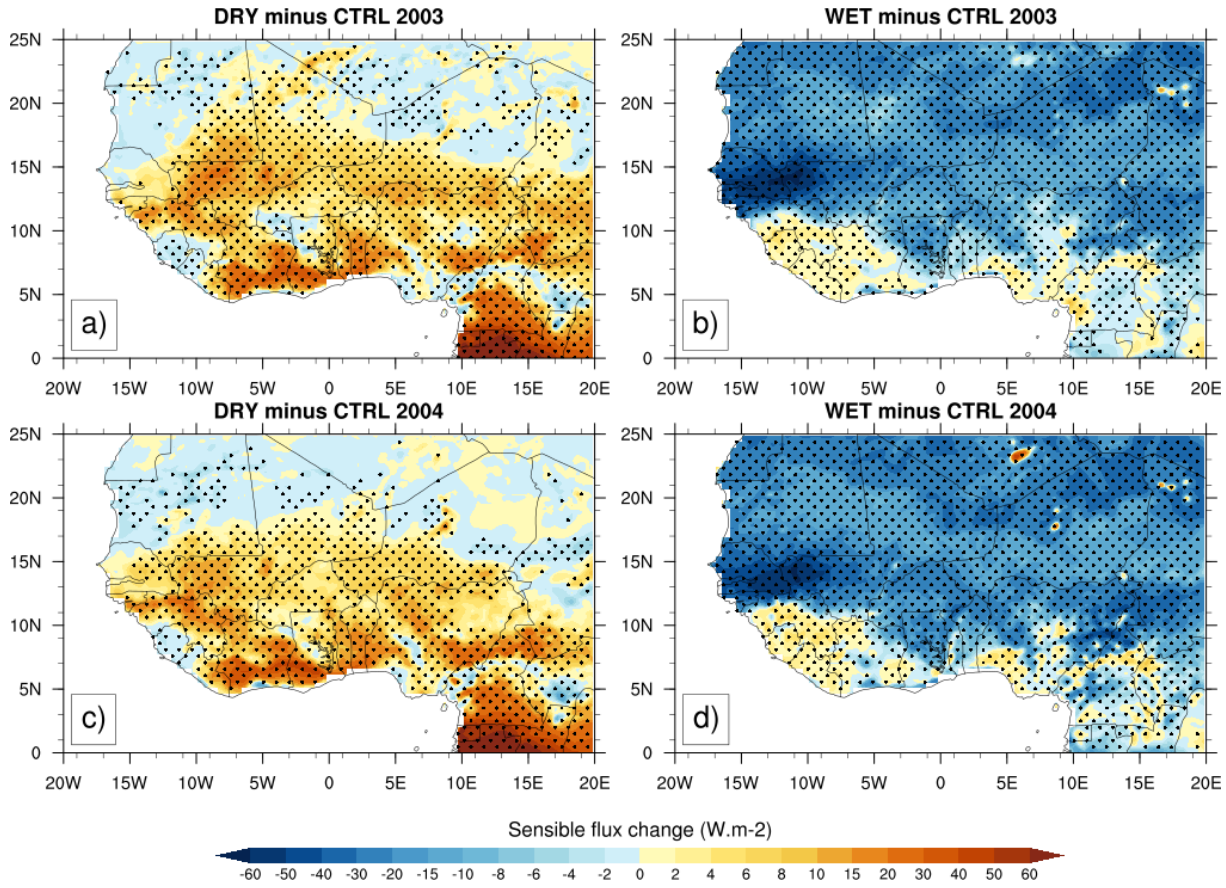


**Figure 14:** Same as Fig.12 but for sensible heat fluxes (in W.m$^{-2}$).

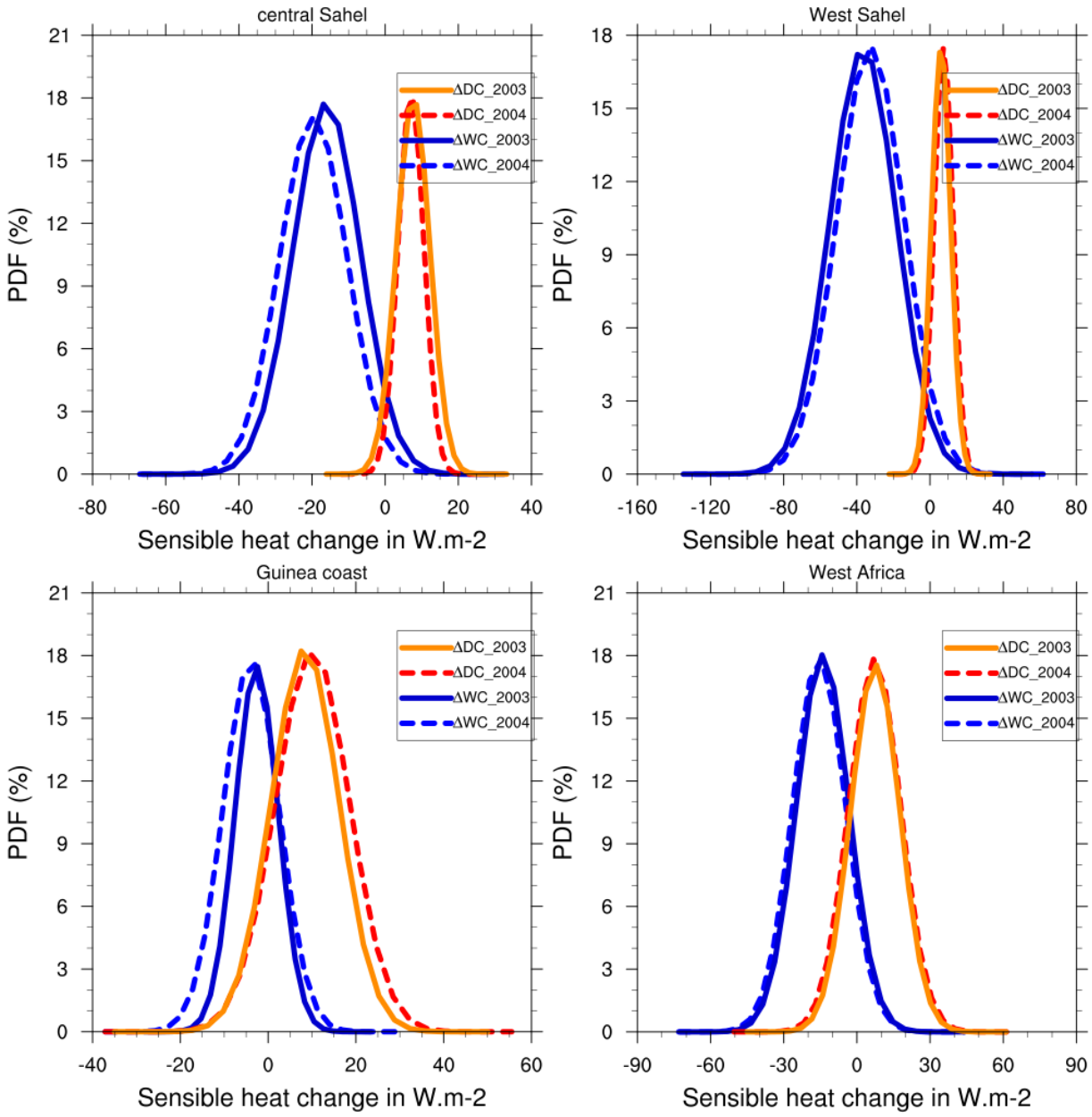


**Figure 15:** Same as Fig.13 but for sensible heat fluxes (in W.m$^{-2}$).

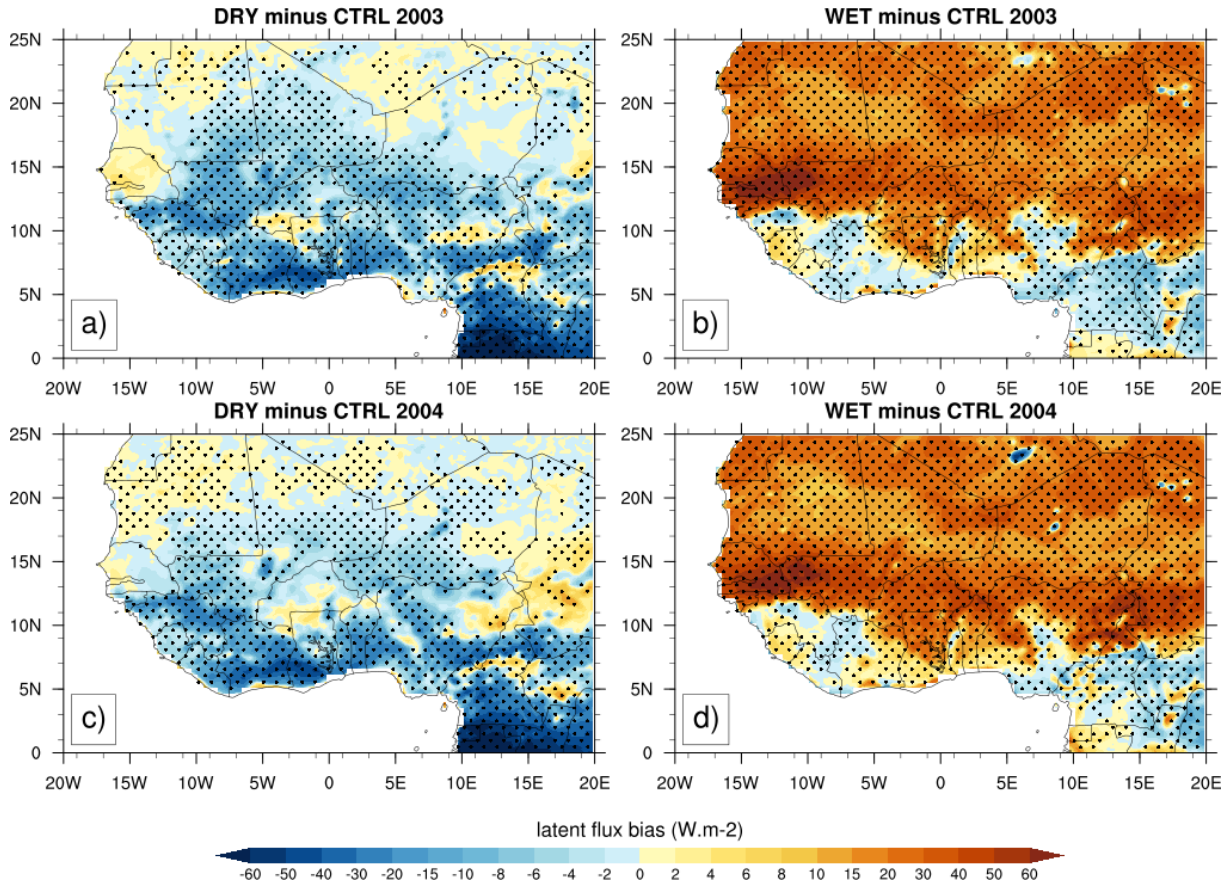


**Figure 16:** Same as Fig.12 but for latent heat fluxes (in W.m$^{-2}$).

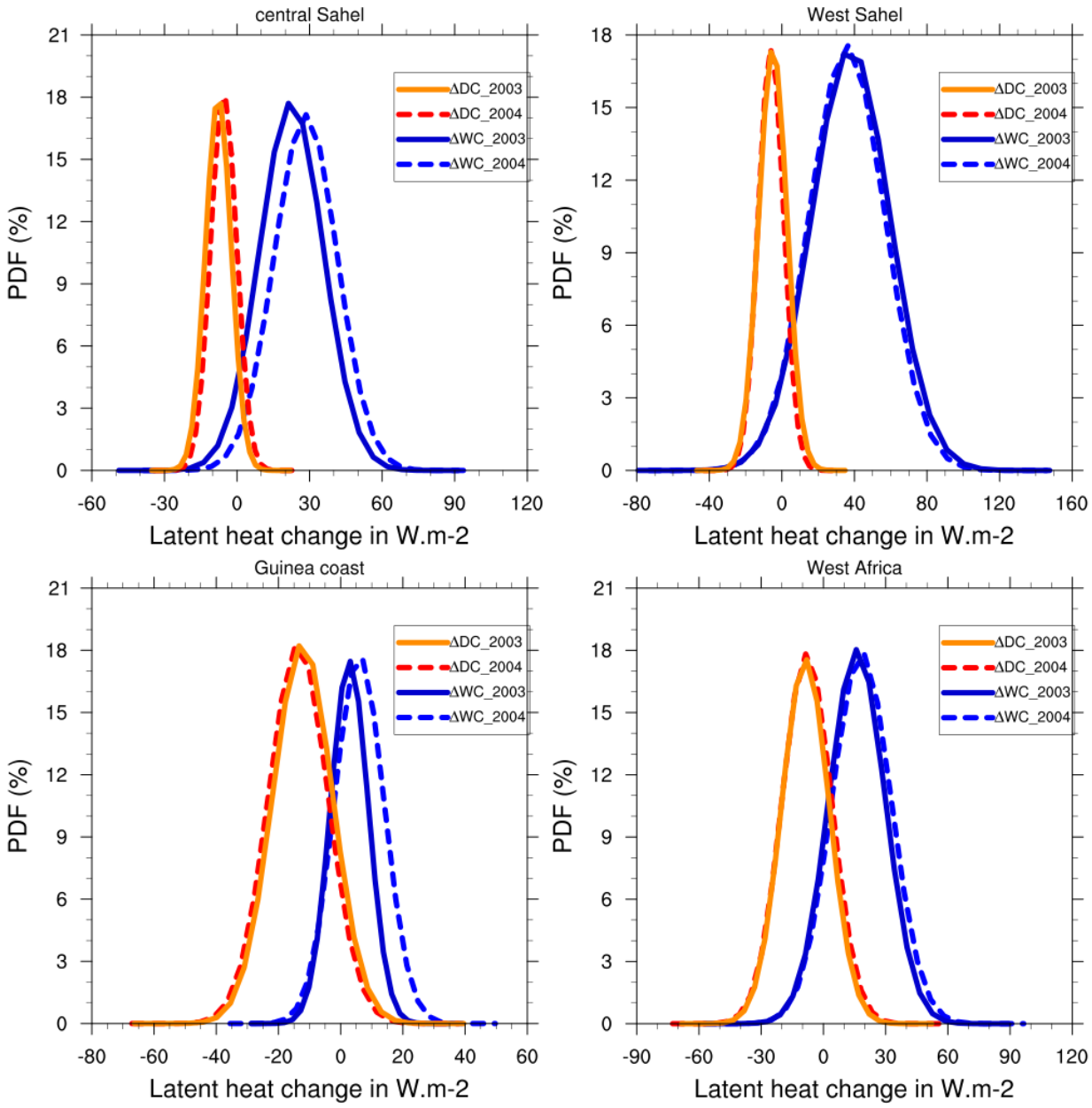


**Figure 17:** Same as Fig.13 but for latent heat fluxes (in $W.m^{-2}$).

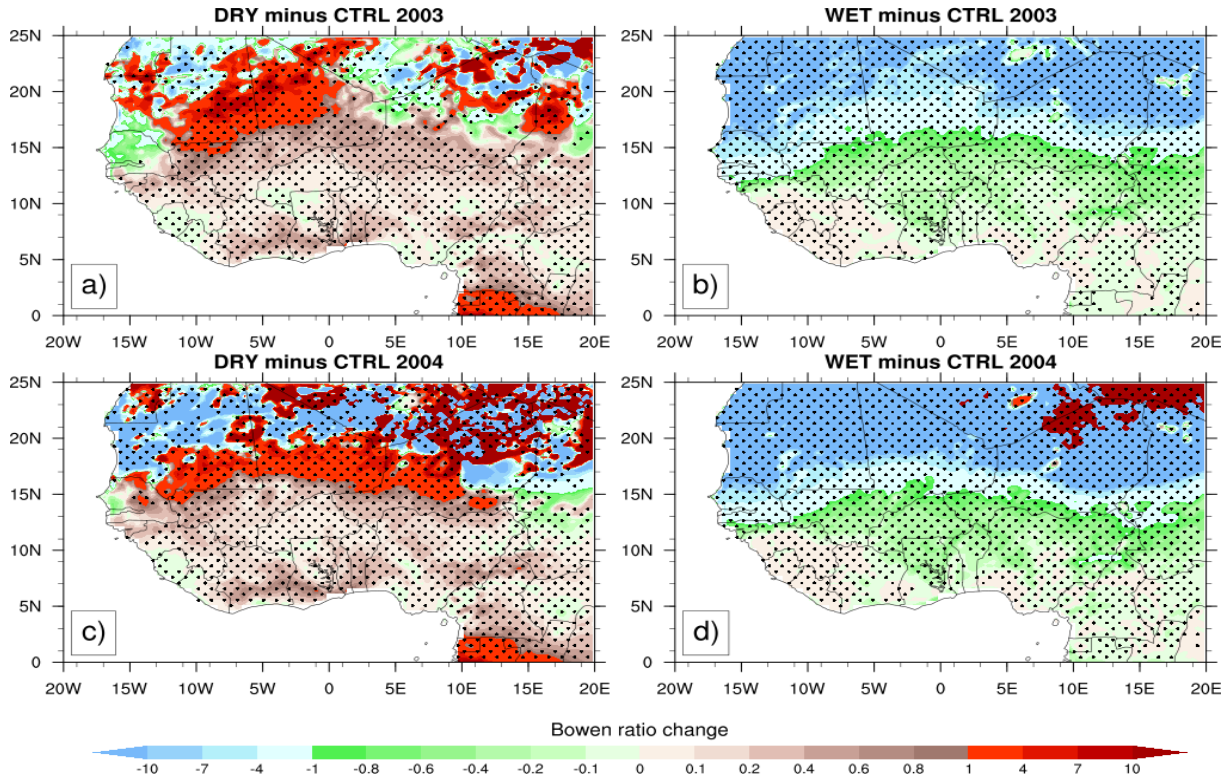


**Figure 18:** Same as Fig.12 but for Bowen ratio.

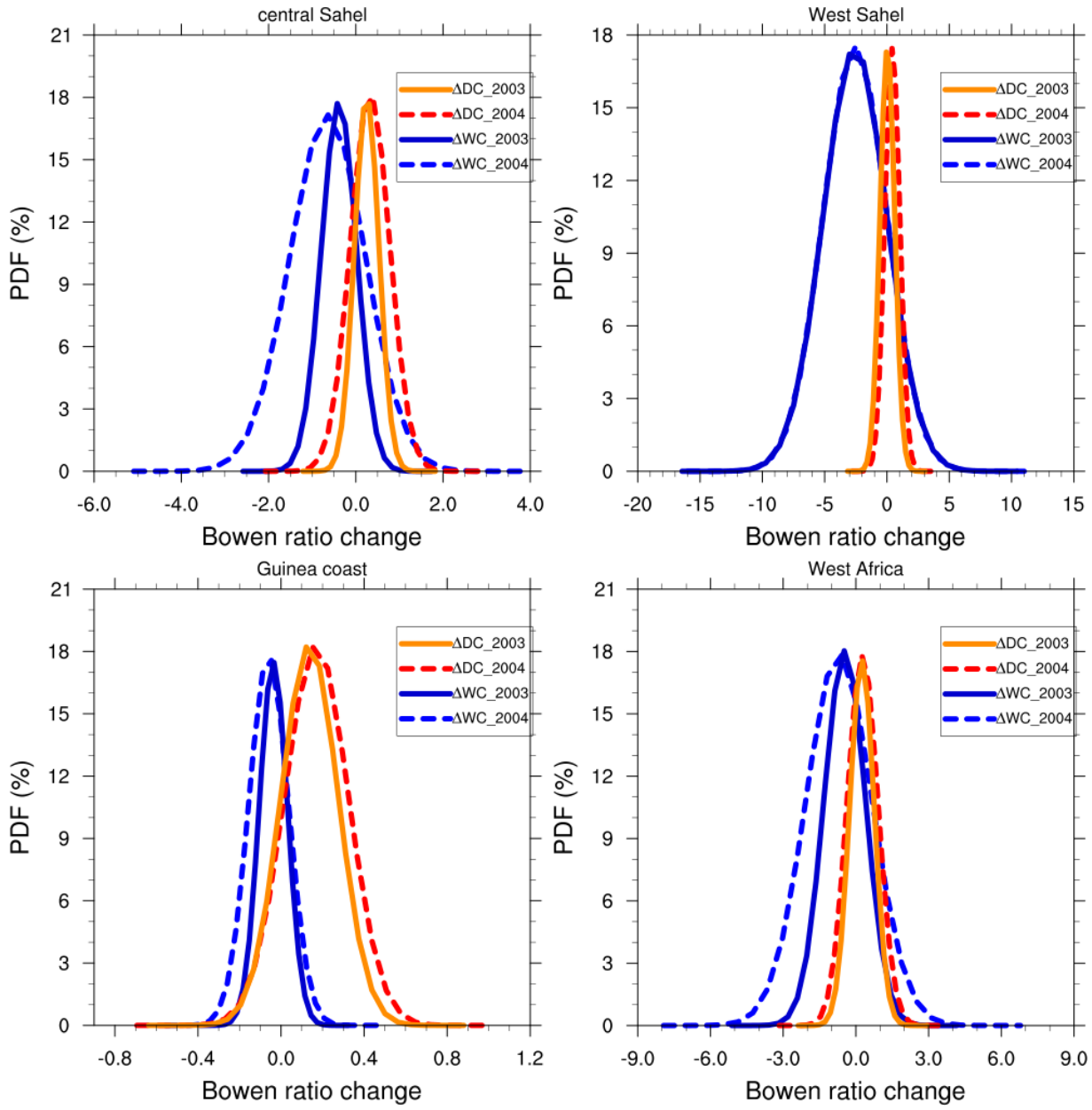


**Figure 19:** Same as Fig.13 but for Bowen ratio.

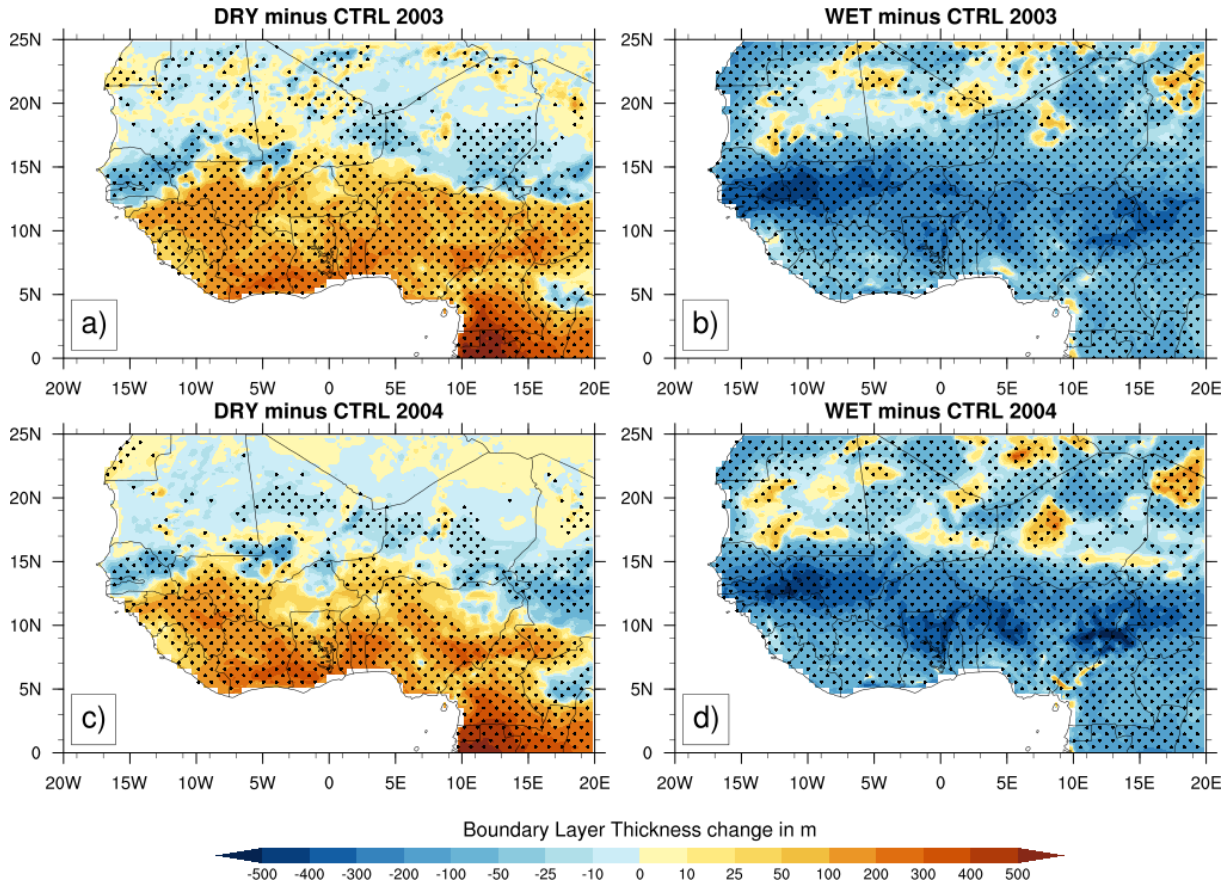


**Figure 20:** Same as Fig.12 but for the change of the height of the planetary boundary layer (in m).

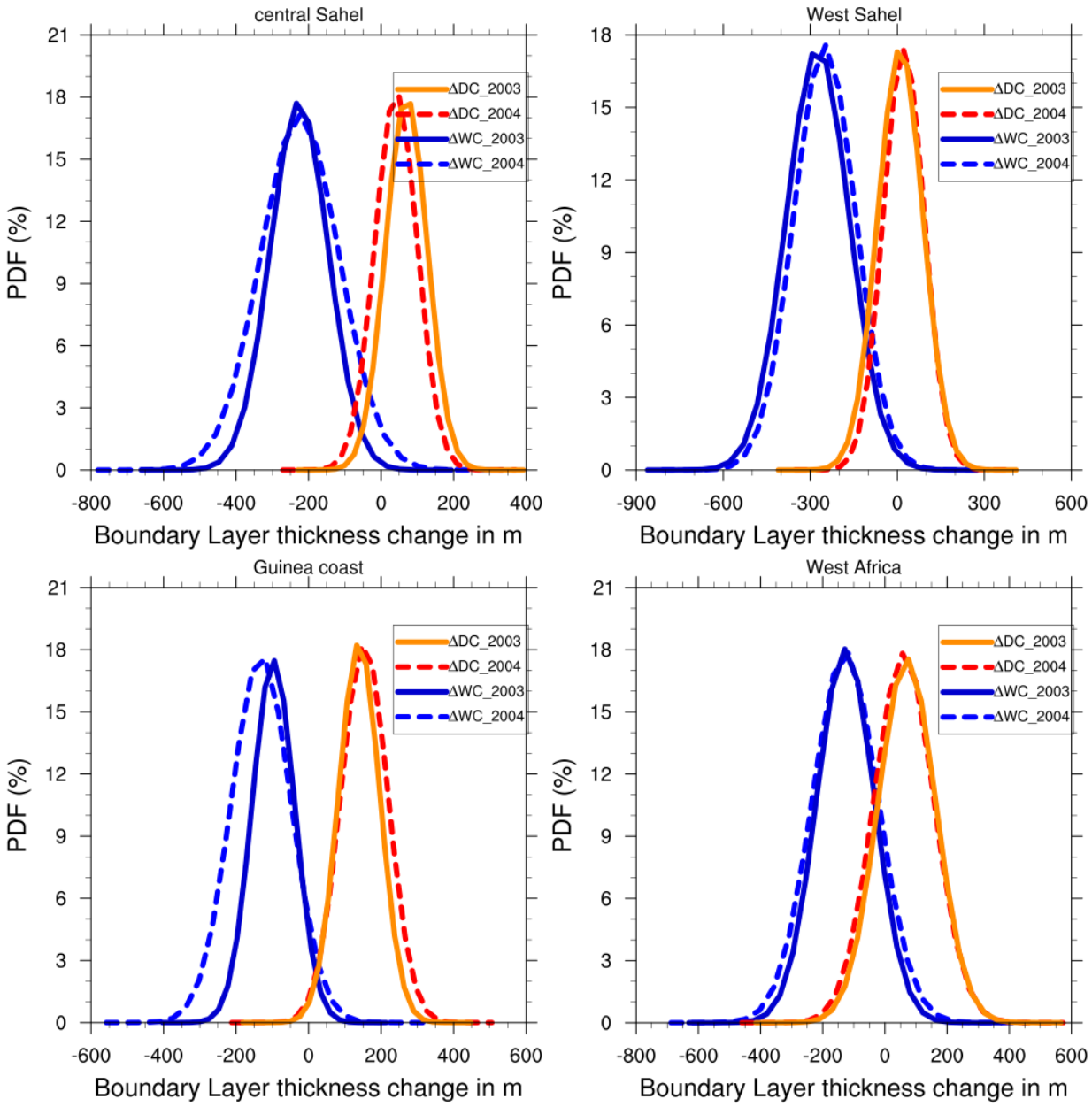


**Figure 21:** Same as Fig.13 but for the height of the planetary boundary layer (in m).